



NSTX Upgrade

Centerstack Casing and Lower Skirt Stress Summary

NSTXU-CALC-133-03-00

Rev 0

February 10, 2012

Prepared By:

Peter Titus, PPPL Engineering Analysis Branch,

Reviewed By:

A.Brooks

A.Zolfaghari

Irving Zatz (For Jim Chrzanowski),
NSTX Cognizant Engineer

PPPL Calculation Form

Calculation # **NSTXU-CALC-133-03-00** Revision # 00
#, 0029,0037

WP

(ENG-032)

Purpose of Calculation: (Define why the calculation is being performed.)

The purpose of this calculation is to qualify the new centerstack casing and lower support skirt for the Upgrade loads. The stress contributions are generated in this calculation or gathered from other calculations. A stress summation and summary for the centerstack casing is presented and compared with allowables.

References (List any source of design information including computer program titles and revision levels.)

-See the reference list in the body of the calculation

Assumptions (Identify all assumptions made as part of this calculation.)

Referenced calculations include assumptions.

Calculation (Calculation is either documented here or attached)

Attached in the body of the calculation

Conclusion (Specify whether or not the purpose of the calculation was accomplished.)

Stress levels are below the static and fatigue allowables for the Inconel 625 shell. High strength bolts are needed. ASTM A193 B8M class 2 bolts are recommended for all flange bolts, with appropriate preloading (torqued to 75% yield for conventional through bolts - less for the blind tapped holes in the PF1b mandrel). Welds should be the full thickness of the thinner shell segment. The PF1b mandrel is in the main load path that transfers the casing loads to the support skirt. In the fall of 2011, there were no spacers between flanges connected by the studs, and the studs would not load in compression. The studs will not contribute adequately to the moments and compression loads at the base of the casing. It is recommended that tubular spacers be added to the studs. Bolt stresses at the lower casing flange and skirt flanges are significantly stressed (60 to 70 ksi). These should be preloaded high strength bolts. These have an allowable of 62 ksi, so, they are slightly undersized. Peak stress is at the coax opening of the skirt. Increasing the bolt size on either side of the opening should be considered. The shallow thread blind tapped bolt connection of the PF1b mandrel connection to the PF1a mandrel flange doesn't have adequate capacity to manage the last round of Halo loads. Doubling the number of holes is recommended. High strength bolts are recommended in the "softer" 316 flange - this allows a bit higher shear based on the Federal Screw Fasteners Standard. They will also have to be preloaded to take the lateral load in friction and to develop a greater moment carrying capacity. Welding on the high strength bolt threads would degrade their capacity. Use of Locktite is recommended.

Loading from the CHI electrical connections have been included in the assessment of the net loads on the casing, but the stresses in the CHI rod and the supports for this rod and the reactions from the bus bar connections have not yet been analyzed because details of these supports are lacking.

Cognizant Engineer's printed name, signature, and date

Irving Zatz (for Jim Chrzanowski) _____

I have reviewed this calculation and, to my professional satisfaction, it is properly performed and correct.

Checker's printed name, signature, and date:

_____ A. Brooks

_____ A. Zolfaghari

2.0 Table of Contents

Centerstack Casing Stress Summary

	Section.Paragraph
Title Page	1.0
ENG-033 Form	1.1
Table Of Contents	2.0
Executive Summary	3.0
Digital Coil Protection System Input	4.0
Design Input,	5.0
Criteria	5.1
Design Point Spreadsheet Loads	5.2
References	5.3
Material Properties and Allowables	5.4
Photos and Drawings of Components	5.5
Analysis Models	6.0
Global Model	6.1
Pressure Loading	7.0
Normal Operating Vacuum Loading	7.1
Test Vacuum Loading and Buckling	7.2
Heat Balance Results	8.0
Halo Current Results	9.0
Halo Currents In the Casing	9.1
Halo Currents in the CHI Bus Connection	9.2
Inductive Eddy Current Loads	
Mid Plane Disruption, Quench of P1	10.0
VDE's	11.0
Slow Mid Plane Translation and Quench P1 to P2	11.1
P1 to P5 10 ms VDE Fast Quench at P5	11.2
Tile Disruption Loads	12.0
PF Loading Results	13.0
Stress Results from Ref [2]	13.1
Buckling	13.2
Torsional Loading from TF OOP loads	14.0
Seismic Loading Results	15.0
Skirt Stresses	16.0
Lower Casing and Skirt Bolt Stress	17.0
Upper PF1b Flange Bolting and Weld	17.1
Lower PF1b Flange Bolting	17.2
Skirt Upper Flange Bolting	17.3
Skirt Lower Flange Bolting	17.4
Bolt Loads on the Lower Flag Keys	17.5
Appendix A - Email Correspondence On loads, requirements etc.	
Appendix B - Ref [19] Halo reaction loads for the base skirt with the compliance of the G-10 flange modeled.	

3.0 Executive Summary

This is a collection of results from other calculations intended to assess the total stress in the centerstack casing. Some stress calculations have been added beyond the references to complete assessment of the load inventory. Figure 3.0-1 shows the PDR status of the qualification of some of the elements of the casing structure. All of these components and loads have been re-visited in the final design.

The first component of normal operating stress comes from the inner PF analyses [2]. The inner PF coils, PF 1a and b upper are supported by the casing. Net vertical loads for the upper coils PF1a and b may be found in the Design Point spreadsheet [1], load combinations sheet. These are also included in section 5.2 of this calculation. Reference [2] calculates these independently from the 96 equilibria. The TF coils indirectly load the casing as well because the casing is one of the redundant or statically indeterminant load paths that resist the TF out-of-plane loads. The torsional shear stresses in the casing are quantified in the global model calculation, ref [9] and are summarized in section 14.0. During a normal shot, the heat load on the tiles heats up the casing, but there is active cooling at the flanged ends of the casing to protect the Viton seals and PF1b which is very close to the flange. The thermal gradients in the casing and the conical sections of the casing cause stresses that will superimpose on the PF Lorentz load stresses. The heat balance calculation, reference [3], computes the heat transfer throughout the interior of the vessel from plasma heating of tiles and exposed sections of the vessel. Heat is conducted through the centerstack tiles and the inner divertor and reference [3] quantifies the casing temperature. A stress pass is included in the analysis and provides the stress to be added to other loading components.

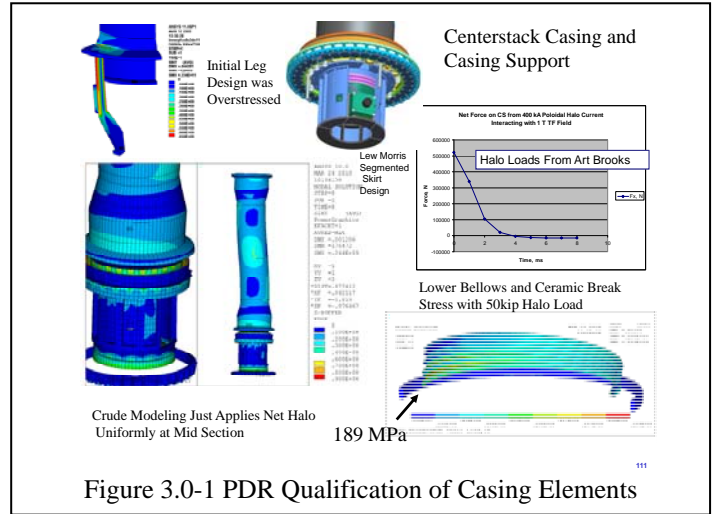
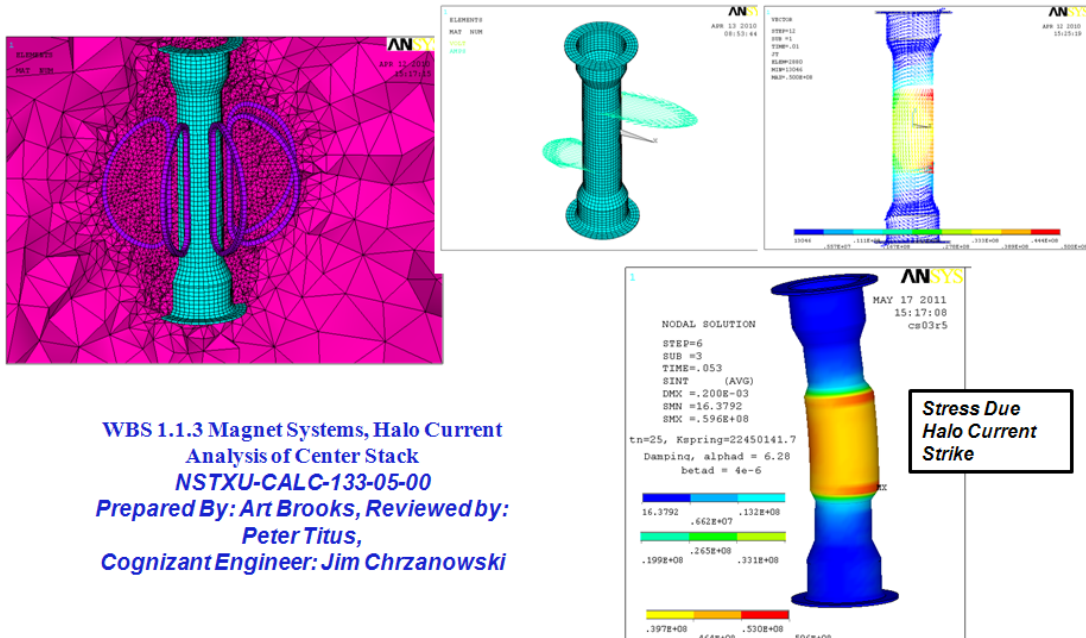


Figure 3.0-1 PDR Qualification of Casing Elements

The Tall Narrow Centerstack Could Experience Excessive Lateral Loads If Peaking Factors are Sustained.



WBS 1.1.3 Magnet Systems, Halo Current
 Analysis of Center Stack
 NSTXU-CALC-133-05-00
 Prepared By: Art Brooks, Reviewed by:
 Peter Titus,
 Cognizant Engineer: Jim Chrzanowski

Figure 3.0-2 Stress due to Halo Currents

Disruption loads are addressed in reference [4] for halo currents and reference [10] for the inductively driven axisymmetric stresses in the casing wall. Inductive current stresses are less than 50 MPa. The halo current loads represent a potentially complex set of loads that depend on the entry and exit points, described in the GRD. They also depend on loading time durations that preclude resistive re-distribution of the non-axisymmetric halo currents for very fast disruptions, and allow resistive re-distribution for slow disruptions. The non-axisymmetric loading that results from the fast disruptions loads the casing dynamically and is addressed by a transient structural calculation. The casing inertia and the spring restraint provided by the bellows limits the stress in the casing. Tile weights used for the inertial components of the model come from the tile stress calculation, ref [6], and the bellows analysis that provided the stiffness, reference [5]. Loads at the bellows spring are a part of the bellows loading addressed in the bellows stress calculation, reference [5]. The bellows spring rate and the cantilever stiffness of the centerstack is an important component of the magnetic stability analysis performed in reference [7]. The centerstack casing is vertically cantilevered from the pedestal. Stresses due to seismic overturning loads may be found in reference [12].

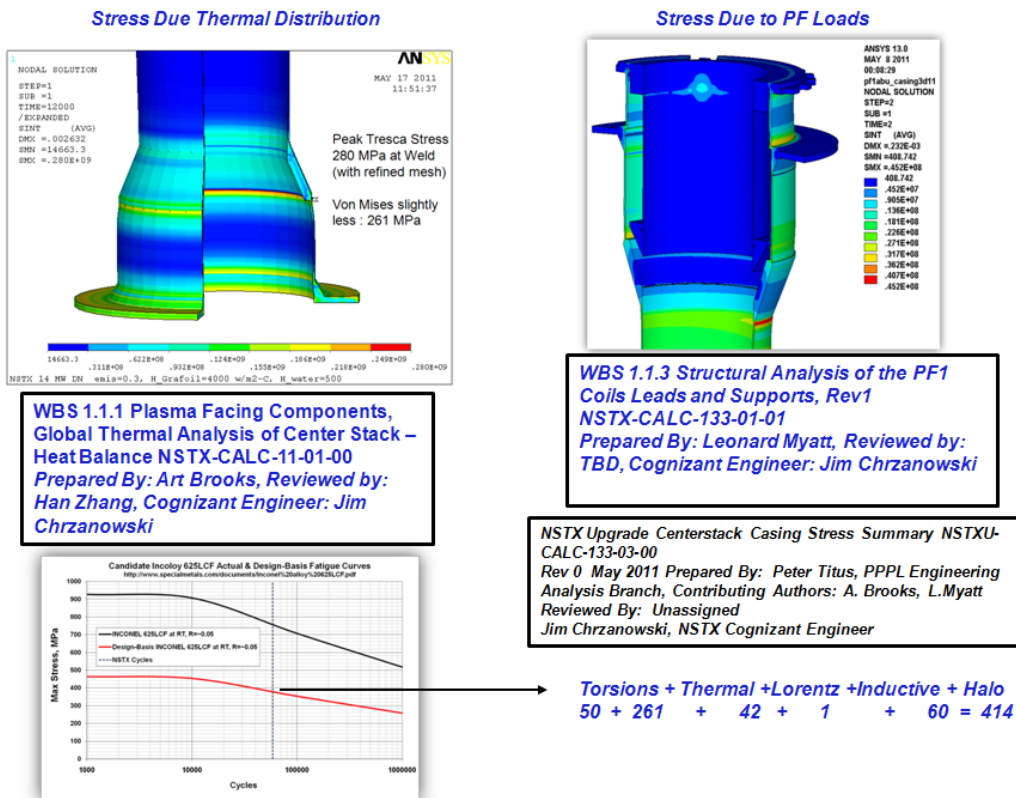


Figure 3.0-3 FDR Presentation Showing Two of the Many Load Components on the Centerstack Casing.

Table 3.0-1 Centerstack Casing Stress Summary (stresses in MPa)

	Calc	Ref	Intersection of 1/4 " shell and 7/16 Flare (Upper)	Equatorial Plane	Intersection of 1/4 " shell and 7/16 Flare (Lower)	Intersection of .438" shell and 7/16 Flare (Lower)	Midle of Flare With Stress concentration of 3 for Coolant Tubes
Vacuum Pressure	7.1		6.3	6.3	6.3	6.3	3
Thermal	8.0		63	0	63	192	120
Halo Stress	9.0		16	48.7	16	16	5
Mid Plane Disruption	10.0		2	10	2	1	1
P1-P2 Disruption	11.0		1	1	1	1	1
Tile Moments	12.0		40	0	40	38	38
PF1a,bU Lorentz	13.1	[2]	45.2	27	45.2	27	18
Normal Op EQ79	14.0		14	18	14	14	3
Seismic	15.0	[12]	4	7	14	4	6
Totals			191.5	118	201.5	299.3	195
F.S based on 625 RT Bending							
Allowable of 450 Mpa			2.349869452	3.8135593	2.23325062	1.503508186	2.307692308
F.S based on 625 RT							
SN Allowable of 380 Mpa			1.984334204	3.220339	1.885856079	1.269629135	1.948717949
(See Figure 5.4-1)							

For the FDR, an envelope of the stresses was presented and the sum was reported as 414 MPa, which was close to the fatigue allowable for Inconel 625. In table 3.0-1, the stresses are summed at four locations and the peak total is 299.3 MPa. This occurs at a weld in the casing, shown in Figure 5.5-3. The weld is a full penetration through the thinner section and backed with a 1/16th-inch seal weld. The stress calculations capture the stress in the full penetration weld. As long as this meets acceptance criteria, the 1/16" weld is redundant.

The possibility of buckling the 1/4 inch casing shell is addressed in ref [2] and additionally in section 13.2 of this calculation.

Bolts at the lower casing flange and skirt flanges are significantly stressed (60 to 70 ksi). These should be preloaded high strength bolts. ASTM A193 B8M class 2 bolts are recommended. These have an allowable of 62.5 ksi, so, they are slightly undersized. Peak stress is at the coax opening of the skirt. Increasing the bolt size on either side of the opening should be considered.

The PF1b mandrel is in the main load path that transfers the casing loads to the support skirt. Currently, there are no spacers between flanges connected by the studs, and the studs will not load in compression. The studs will not contribute adequately to the moments and compression loads at the base of the casing. It is recommended that tubular spacers be added to the studs. Ref [7] calculates the stress due to an offset between the magnetic and structural centers due to tolerances. From [7], the stress due to the manufacturing tolerance would be a maximum of 0.43 MPa and the bellows stress would be 9.77 MPa.

Recent questions regarding the halo current loading on the centerstack casing highlights a design weakness in the support of the casing. The upper bellows provides minimal lateral restraint, and the casing is basically cantilevered from the lower structures and bolt circles. Halo Loads and, particularly, moments were acceptable when credit was taken for mitigation of the peaking factor from dynamic effects and resistive redistribution of the asymmetric currents. From October 2011 emails, there is a large uncertainty in the halo loads - Art Brooks suggests enveloping the uncertainty by assuming the worst loading at the mid plane of 50,000 lbs. This would produce a moment of $50000 * (1.6m * 39.37 + 22in) = 4.2e6$ in-lbs. The skirt bolt pattern has a section modulus of 19 in^3 and the bolt stress would be 237,000 psi. The bolts to the g-10 ring, and to the inserts in the TF flags, and connection through the lower crown to the pedestal, would also see high loads.

It was recommended that a lateral restraint be added at the upper bellows elevation - a slip ring or struts. They would have to take half the 50000 lb halo load. This would much reduce the moment at the base and add needed margin against loading that probably won't be able to be quantified until the upgrade has operated. Art Brooks recalculated the reaction loads and moments at the base (Appendix B).

Updated Halo loading of the lower G-10 ring and its connections to the TF flags, is evaluated in ref [20].

4.0 Digital Coil Protection System (DCPS) Input

Casing Stress:

Most of the loading on the casing is either thermal or disruption loading. The DCPS typically is concerned mainly with coil Lorentz force derived stresses. Table 3.0-1 lists the Lorentz Force derived stress as 45 MPa. It occurs at the intersection of the straight section and flare. This comes from L. Myatt's calculation of the casing stresses from the inner PF coils, ref [2]. The 45 MPa will scale based on the net vertical load from PF1a and b upper. Myatt used the worst of the 96 scenarios, which corresponds to the 67939 lbs from the design point spreadsheet - excerpt at right. The DCPS should compute the casing Lorentz Stress from:

Fz(lbf)	PF1aU+PF1bU
Min w/o Plasma	-29865
Min w/Plasma	-67939
Min Post-Disrupt	-35071
Min	-67939
Worst Case Min	-182214
Max w/o Plasma	55989
Max w/Plasma	48336
Max Post-Disrupt	46450
Max	55989
Worst Case Max	257587

(Sum of PF1a and b Vertical loading in lbs) * 45MPa /67939lbs = Lorentz Stress

The max stress in the casing is 200 MPa for 96 equilibria, plus thermal and disruption loads. With the Lorentz portion of the stress at 45 MPa, the "headroom" needed for Non-Lorentz Loads is 155 MPa.

The static allowable is 450 MPa so the Lorentz stress could go to 300 MPa, and still pass the static allowable. The worst case Max load is 257587lbs - this would produce a casing stress of $257587/67939 * 45 = 170$ MPa - so there is only marginally a possibility that currents in their worst configuration could cause an unacceptable stress - but the bolting in the lower flange will fail before this stress could be reached.

Lower Casing Support Bolts

Because they are sized to the worst halo loads, there isn't much margin to take anything more than the total PF 1a,b upper and lower Lorentz launching load that was used in section 17 to qualify the bolts. This is 25161 lbs from Table 5.2-1. Maintaining the net PF1a,b upper and lower summation below this value will protect the bolting from halo loads during a disruption. If more margin is needed to allow a better operating window, the halo loads on the bolts will have to be re-visited.

5.0 Design Input,

5.1 Criteria

Criteria may be found in reference [8], NSTX Structural Design Criteria Document, I. Zatz.

5.2 Design Point Spreadsheet Loads

Reference [2] addresses the stress in the centerstack due to the loads from PF1a and b upper. The bolting at the lower end of the casing assembly is exposed to the net loads from PF1a, and b, upper and lower. This summation is available in the Design Point spreadsheet, reference [1].

Table 5.2-1 Net Vertical Loads on the Lower Connections of the Skirt

Fz(lbf)	(PF1aU+PF1bU)+(PF1aL+PF1bL)
Min w/o Plasma	-30569
Min w/Plasma	-44386
Min Post-Disrupt	-31373
Min	-44386
Worst Case Min	-71465
Max w/o Plasma	25161
Max w/Plasma	15513
Max Post-Disrupt	24002
Max	25161
Worst Case Max	363517

Table 5.2-2 Net Vertical Loads on the Lower Connections of the Skirt Plus OH Coil

Fz(lbf)	(PF1AU+PF1BU+PF1BL+PF1AL+OH)
Min w/o Plasma	-39635
Min w/Plasma	-53445
Min Post-Disrupt	-41843
Min	-53445
Worst Case Min	-375500
Max w/o Plasma	20397
Max w/Plasma	10748
Max Post-Disrupt	19630
Max	20397
Worst Case Max	375501

Fz(lbf)	PF1aU+PF1bU
Min w/o Plasma	-29865
Min w/Plasma	-67939
Min Post-Disrupt	-35071
Min	-67939
Worst Case Min	-182214
Max w/o Plasma	55989
Max w/Plasma	48336
Max Post-Disrupt	46450
Max	55989
Worst Case Max	257587

5.3 References

- [1] http://www.pppl.gov/~neumeyer/NSTX_CSU/Design_Point.html Dated 2 -17- 2009
- [2] WBS 1.1.3 Structural Analysis of the PF1 Coils Leads and Supports, Rev1 NSTX-CALC-133-01-01 Prepared By: Leonard Myatt, Reviewed by: TBD, Cognizant Engineer: Jim Chrzanowski
- [3] WBS 1.1.1 Plasma Facing Components, Global Thermal Analysis of Center Stack – Heat Balance NSTX-CALC-11-01-00 Prepared By: Art Brooks, Reviewed by: Han Zhang, Cognizant Engineer: Jim Chrzanowski
- [4] WBS 1.1.3 Magnet Systems, Halo Current Analysis of Center Stack NSTXU-CALC-133-05-00 Prepared By: Art Brooks, Reviewed by: Peter Titus, Cognizant Engineer: Jim Chrzanowski
- [5] Bellows Qualification Calc # NSTXU CALC 133-10-00, Peter Rogoff
- [6] Tile Stress Analysis (ATJ) NSTXU CALC 11-03-00, Art Brooks Used to include tile weights into the effective density of the centerstack casing, transmitted via email:
Peter, Pete: Attached are the volumes Ankita extracted from the ProE models. The density of the Center Case (inconel) is 8440 kg/m³, the tile (ATJ Graphite - www.graftech.com) is 1760 kg/m³ giving a total mass of 1138 kg and an effective density if the CS (which includes the mass of the tiles) of 12,248 kg/m³.
- [7] OH & PF1 & 2 Electromagnetic Stability Analyses NSTXU-CALC-133-11-00 Rev 0 March 2 2010 Prepared By: Peter Titus, , Reviewed By: Ali Zolfaghari Cognizant Engineer: Jim Chrzanowski WBS 1.1.3
- [8] NSTX Structural Design Criteria Document, NSTX_DesCrit_IZ_080103.doc I. Zatz
- [9] NSTX-CALC-13-001-00 Rev 1 Global Model – Model Description, Mesh Generation, Results, Peter H. Titus June 2011
- [10] WBS 1.1.1 Disruption Analysis of Passive Plates, Vacuum Vessel & Components NSTXU-CALC-12-01-01 Rev 1 April, 2011 Prepared By: Peter Titus, Contributing Authors: A. Brooks, Srinivas Avasarala, J. Boales Reviewed By: Yu Hu Zhai, Cognizant Engineer: Peter Titus
- [11] National Spherical Torus Experiment NSTX CENTER STACK UPGRADE GENERAL REQUIREMENTS DOCUMENT NSTX_CSU-RQMTS-GRD Revision 0 March 30, 2009 Prepared By: Charles Neumeyer NSTX Project Engineering Manager
- [12] NSTX Upgrade Seismic Analysis NSTXU-CALC-10-02-00 Rev 0 February 9 2011 Prepared By: Peter Titus, reviewed by F. Dahlgren
- [13] Analysis of the NSTX Upgrade Centerstack Support Pedestal NSTXU-CALC-12-09-00 May 2011 WBS 1.1.2 Prepared By: Peter Titus Reviewed By: Ali Zolfaghari, Cognizant Engineer: Mark Smith
- [14] MODELLING OF THE TOROIDAL ASYMMETRY OF POLOIDAL HALO CURRENTS IN CONDUCTING STRUCTURES N. POMPHREY, J.M. BIALEK_, W. PARK, Princeton Plasma Physics Laboratory, Princeton University, Princeton, New Jersey,
- [15] Email from Art Brooks Thu 3/11/2010 8:21 AM, providing Upper and Lower design loads for the centerstack casing halo loads, copy of the email is included in the appendices
- [16] NSTX Basic Tile Analysis Qualification NSTX-CALC-11-02-00 December 2010 Prepared By: J. Boales
- [17] "General Electric Design and Manufacture of a Test Coil for the LCP", 8th Symposium on Engineering Problems of Fusion Research, Vol III, Nov 1979
- [18] "Handbook on Materials for Superconducting Machinery" MCIC- HB-04 Metals and Ceramics Information Center, Battelle Columbus Laboratories 505 King Avenue Columbus Ohio 43201
- [19] email from Art Brooks November 1 2011, providing Halo reaction loads for the base skirt with the compliance of the G-10 flange modeled.
- [20] STRUCTURAL CALCULATION OF THE TF FLAG KEY, Rev 1 NSTXU-CALC-132-08-01 December 05, 2011 Prepared By: Ali Zolfaghari
- [21] Progress on CHI and MGI Experiments on NSTX R. Raman, 53rd Meeting of the Division of Plasma Physics, APS 2011 Conference November 14-18 2011 Salt Lake City
- [22] FED-STD-H28 Federal Standard Screw Thread Standards for Federal Services FED-STD-H28 March 31 1978
- [23] NSTX Upgrade OH Coaxial Cable and Embedded Leads NSTXU-CALC-133-07-00 September 7 2011 Prepared By: Michael Mardenfeld, PPPL Mechanical Engineering

5.4 Material Properties and Allowables

Table 5.4-1 Tensile Properties for Stainless Steels

Material	Yield, 292 deg K (MPa)	Ultimate, 292 deg K (MPa)
316 LN SST	275.8[17]	613[17]
316 LN SST Weld	324[17] (23.3ksi)	482[17] 553[17]
316 SST Sheet Annealed	275[18]	596[18]
316 SST Plate Annealed		579
304 Stainless Steel (Bar,annealed)	234 33.6ksi	640 93ksi
304 SST 50% CW	1089	1241 180ksi

Table 5.4-2 Coil Structure Room Temperature (292 K) Maximum Allowable Stresses, S_m = lesser of 1/3 ultimate or 2/3 yield, and bending allowable=1.5* S_m

Material	S_m	1.5 S_m
316 Stainless Steel	184 MPa, 26.7 ksi	276 MPa
316 Weld	161 MPa	241 MPa
304 Stainless Steel (Bar,annealed)	156MPa(22.6ksi)	234 MPa (33.9ksi)

Weld Allowable

From the NSTX Criteria:

For welds in steel, the design Tresca stress shall be the lesser of:
 2/3 of the **minimum** specified yield if the weld at temperature, or
 1/3 of the **minimum** specified tensile strength of the weld at temperature.

From the AISC Criteria:

Reference and Weld	Rod or weld wire	Parent Material	Allowable Stress (Exclusive of Weld Efficiency)
AISC Stress on cross section of full penetration Welds		All	Same as Base material
AISC Shear Stress on Effective Throat of fillet weld	AWS A5.1 E60XX	A36 -	21 ksi

For shear on an effective throat of a fillet, For 304 Stainless, the weld metal is annealed, or the base metal in the heat effected zone is annealed. and Estimate $241 \cdot 21/36 = 140 \text{ MPa} = 20 \text{ ksi}$ (without weld efficiency)
 This is consistent with NSTX Criteria of 2/3 yield or 2/3 of 30ksi for annealed 304
 With a weld efficiency of .7 the allowable is 14ksi, or 96 MPa
 For fillets divide weld area by $\sqrt{2}$

Figure 5.4-1 Weld Allowable

Inconel 625 properties are shown below and in Figure 5.4.2-. Fatigue allowables from ref [2] are shown in figure 5.4-3

ASTM A193 Bolt Specs from PortlandBolt.com

B8 Class 2 Stainless steel, AISI 304, carbide solution treated, strain hardened

Mechanical Properties

Grade	Size	Tensile ksi, min	Yield, ksi, min	Elong, %, min	RA % min
B8 Class 2	Up to 3/4	125	100	12	35
	7/8 - 1	115	80	15	35
	1-1/8 - 1-1/4	105	65	20	35
	1-3/8 - 1-1/2	100	50	28	45

The ASTM A193 B8M Class 2 5/8 inch Bolts would have a Stress Allowable of the lesser of $125/2$ or $2/3 * 100 = 62.5$ ksi

From Ref 2

Center stack coil support structure is made from Inconel 625:

$S_y \sim 65$ ksi, $S_{ut} \sim 130$ ksi

$S_m \sim 43$ ksi (300 MPa)

Membrane + Bending Stress Limit at RT: $(1.5)300 = 450$ MPa

Max Cyclic Stress (58.5k cycles) = 375 MPa ($R \sim 0.05$)

INCONEL 625			
Test Temperature, °F(°C)	Ultimate Tensile Strength, ksi (MPa)	Yield Strength at 0.2% offset, ksi (MPa)	Elongation in 2" percent
Room	138.8 (957)	72.0 (496)	38
200	133.3 (919)	67.3 (464)	41
400	129.4 (892)	62.2 (429)	44
600	125.6 (866)	59.5 (410)	45
800	122.2 (843)	59.2 (408)	45

Figure 5.4-2 Inconel 625 Properties

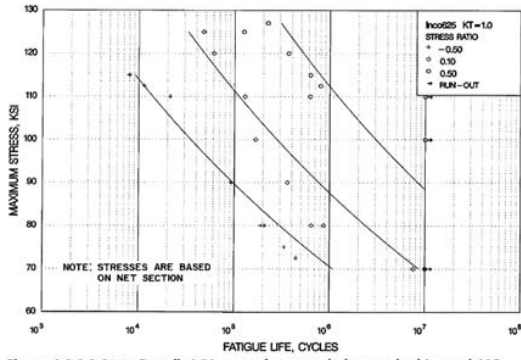
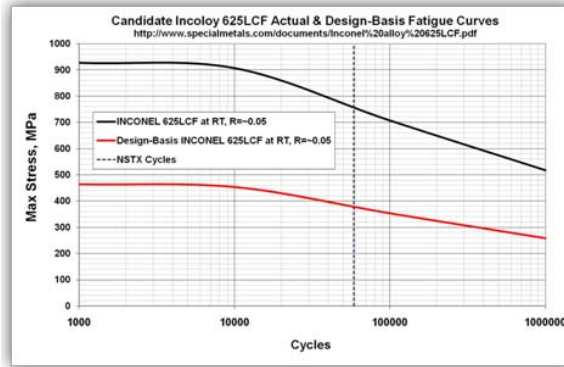


Figure 6.3.3.1.8(a). Best-fit S/N curves for annealed unnotched Inconel 625 bar, longitudinal direction.



Fully Reversed Strain vs. Cycles Incoloy 600

Degrees C	25	95	205	315
10,000 Cycles	.0036	.0043	.0058	.0052
50,000	.0021	.0021	.0026	.0023
100,000	.0018	.0018	.002	0.0018

Figure 5.4-3 Inconel 625 Fatigue Properties

5.5 Photos and Drawings of Components

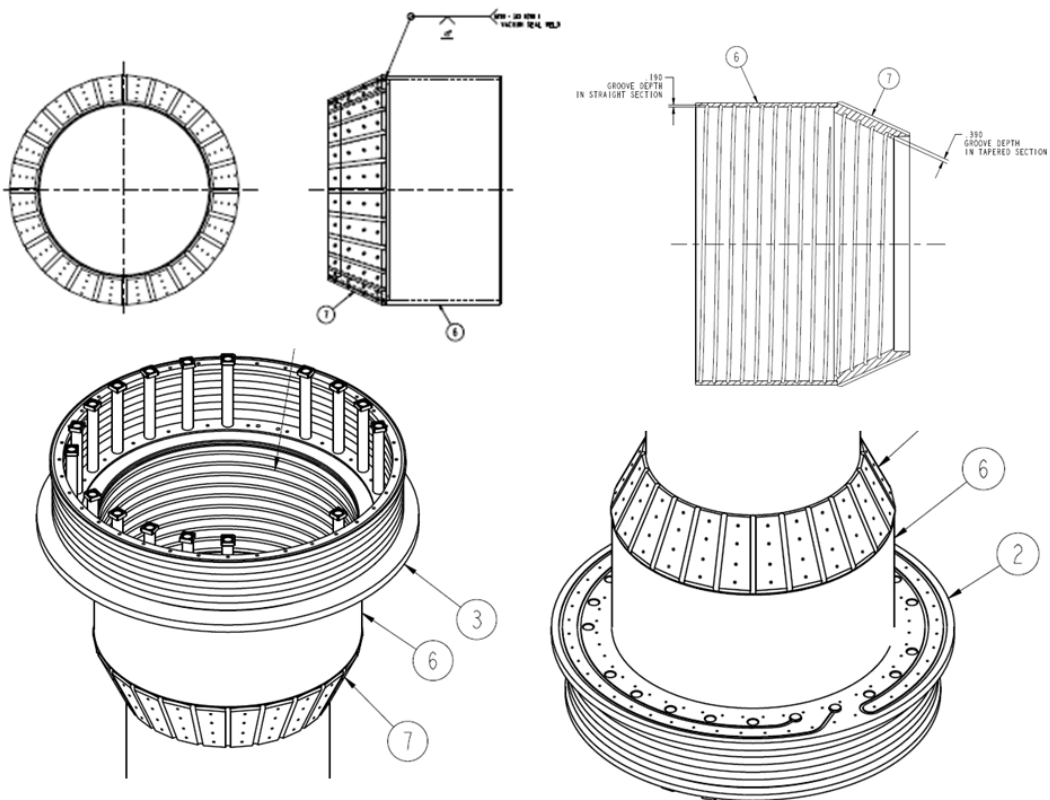
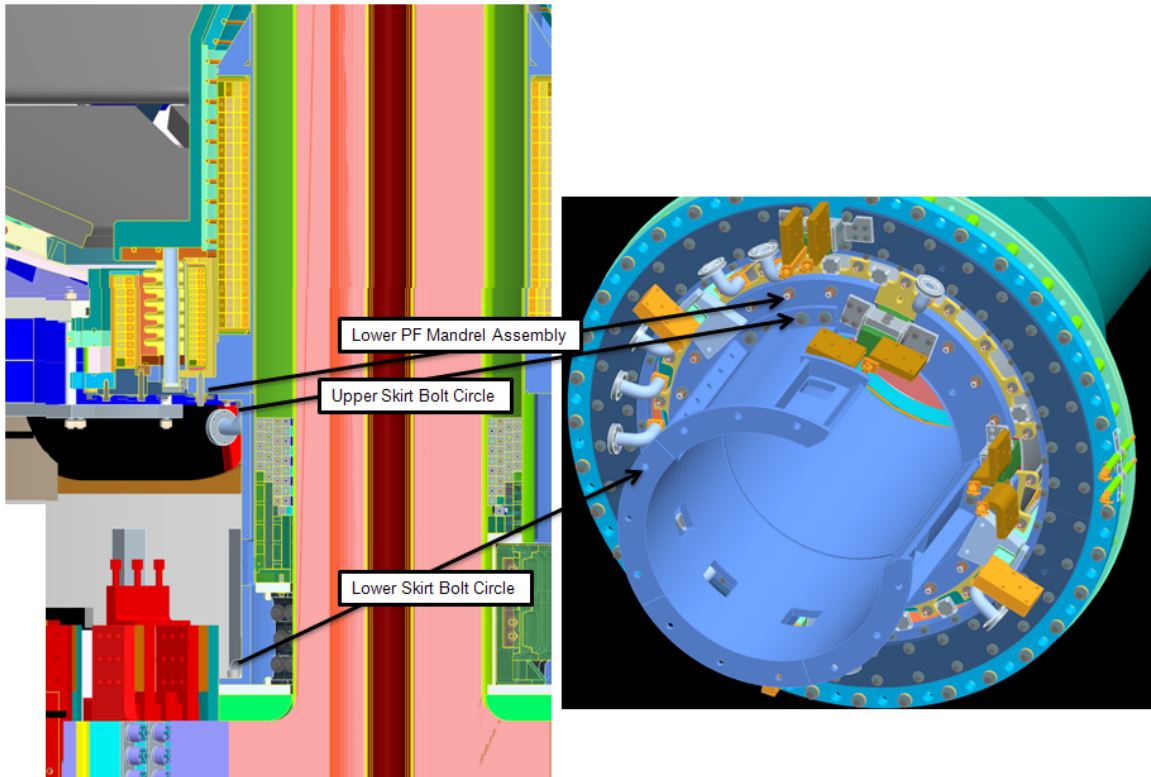


Figure 5.5-1

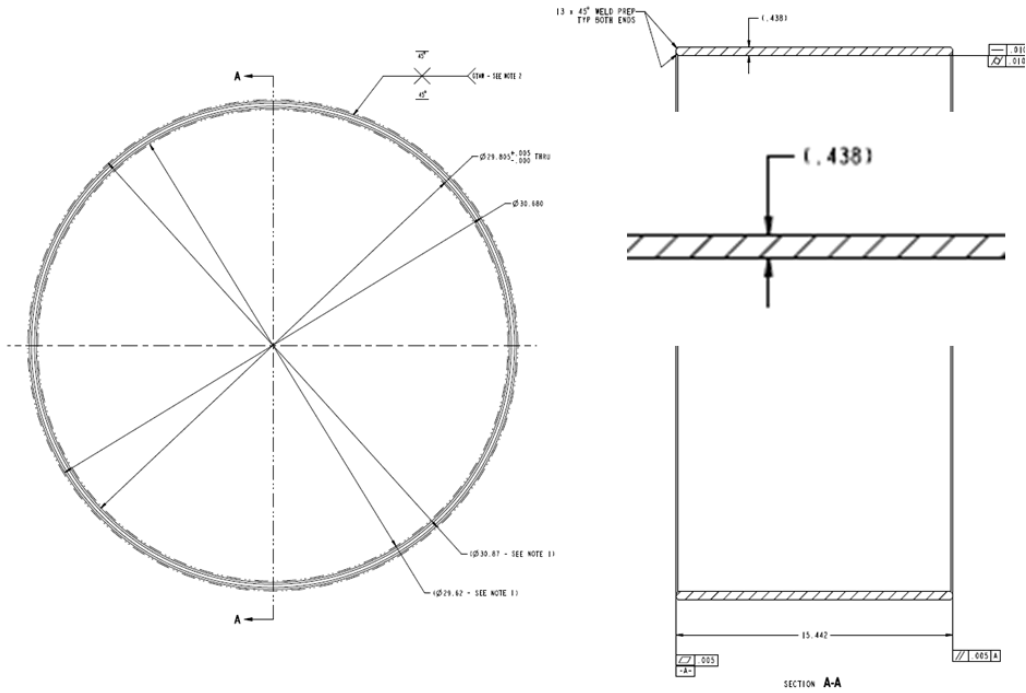


Figure 5.5-2 Upper and Lower Cylindrical Sections

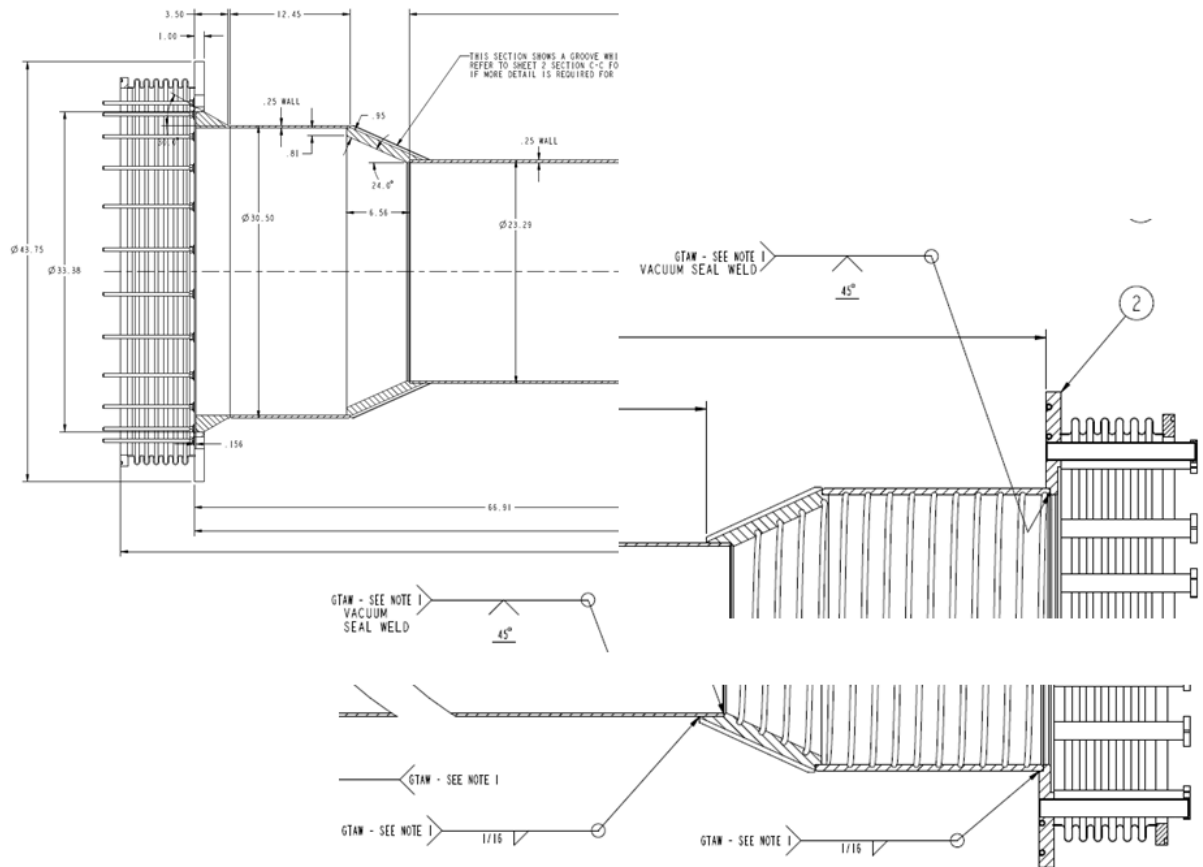


Figure 5.5-3 Casing Dimensions and Weld Details

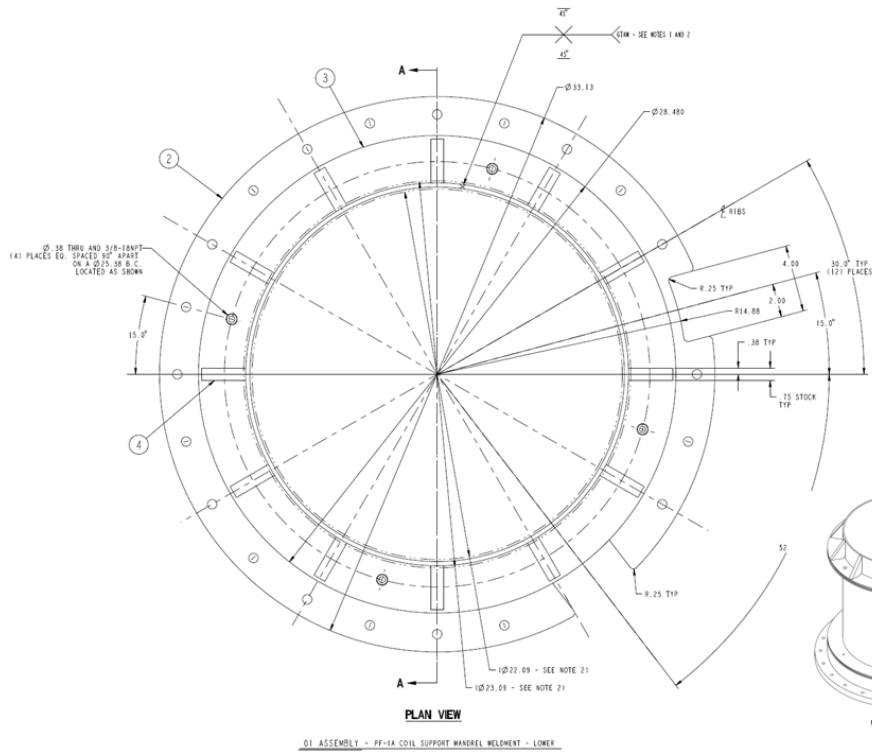


Figure 5.5-4 Lower Mandrel Assembly

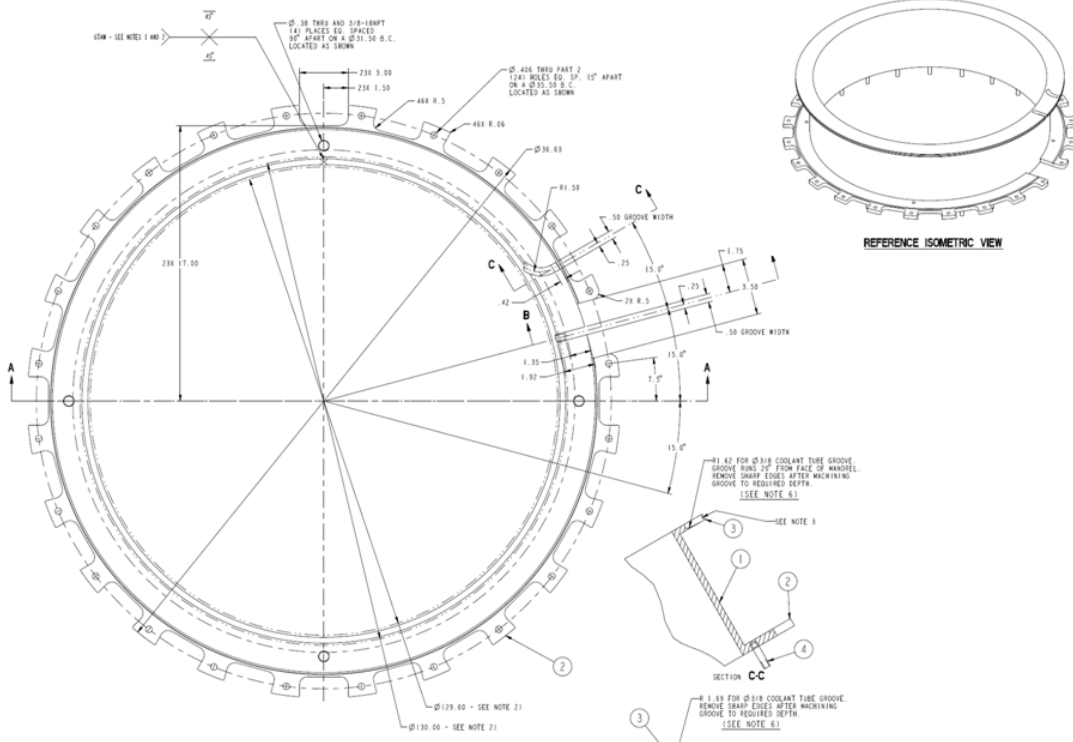


Figure 5.5-5 Lower PFbl Mandrel Assembly

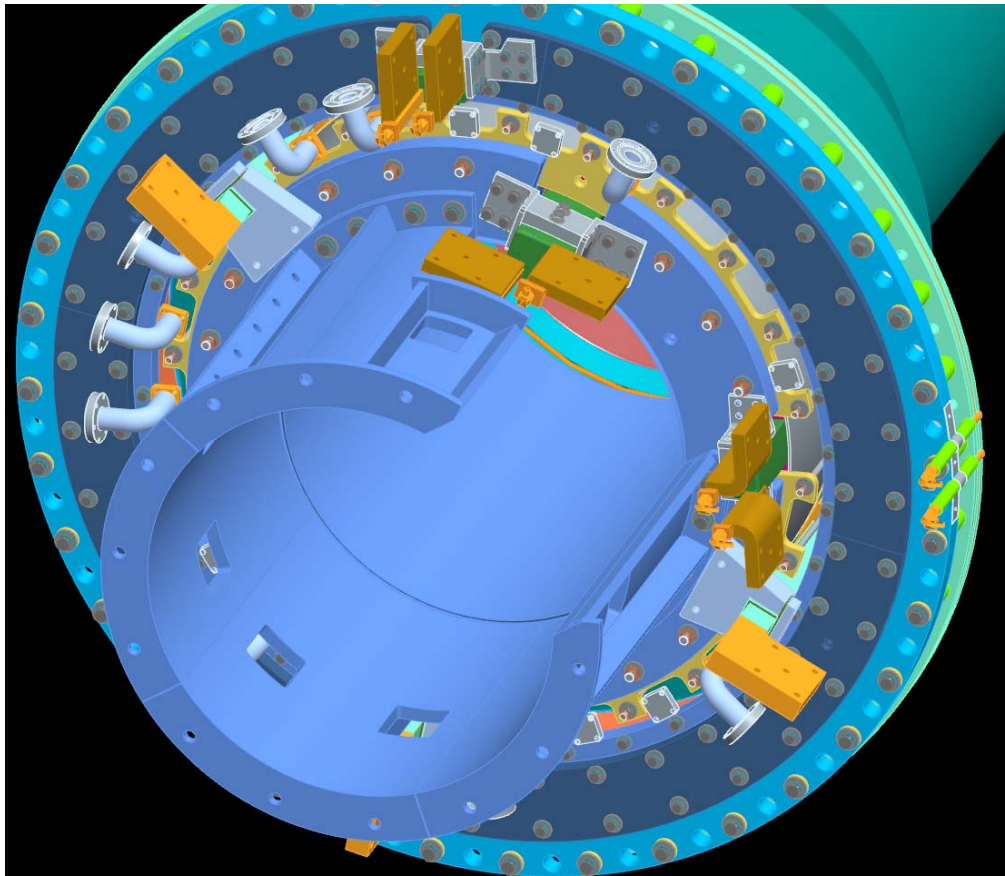


Figure 5.5-6 Lower Mandrel Assembly (October 2011 version with 11 5/8 inch bolts in the lower flange)

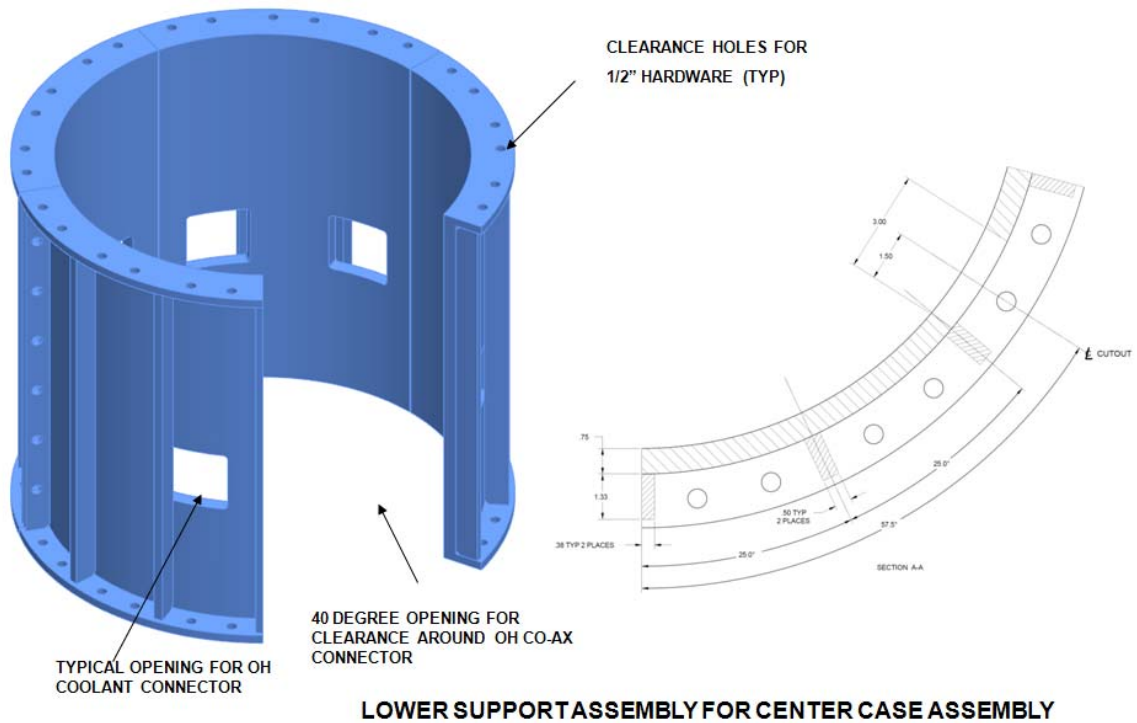


Figure 5.5-7 Lower Support Skirt (FDR vintage with 24 1/2 inch bolts at the lower flange)

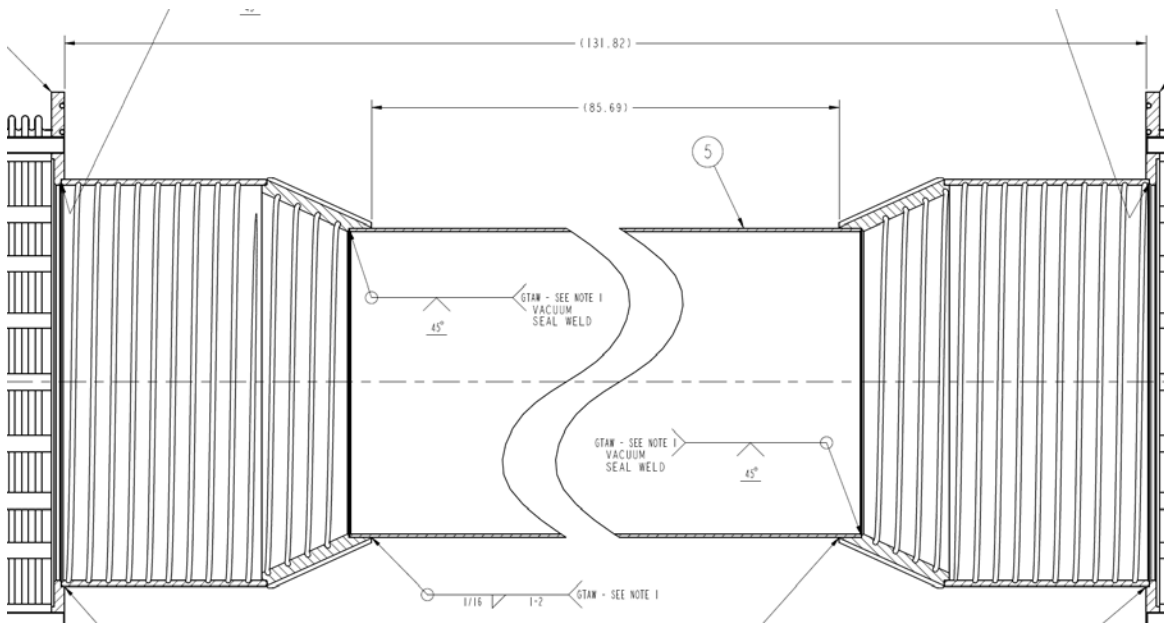


Figure 5.5-8 Upgrade Centerstack Casing Drawing

6.0 Analysis Models

The referenced calculations include a number of separate models for thermal and electromagnetic modeling. The centerstack casing is included in the global calculation, ref[9].

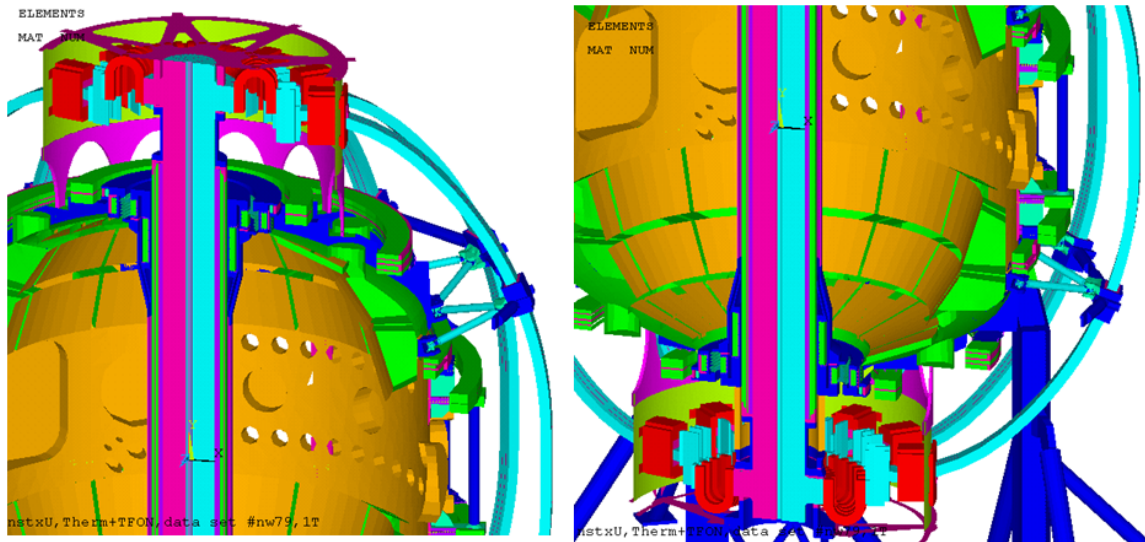


Figure 6.0-1 Global Model Representation of the Centerstack Casing

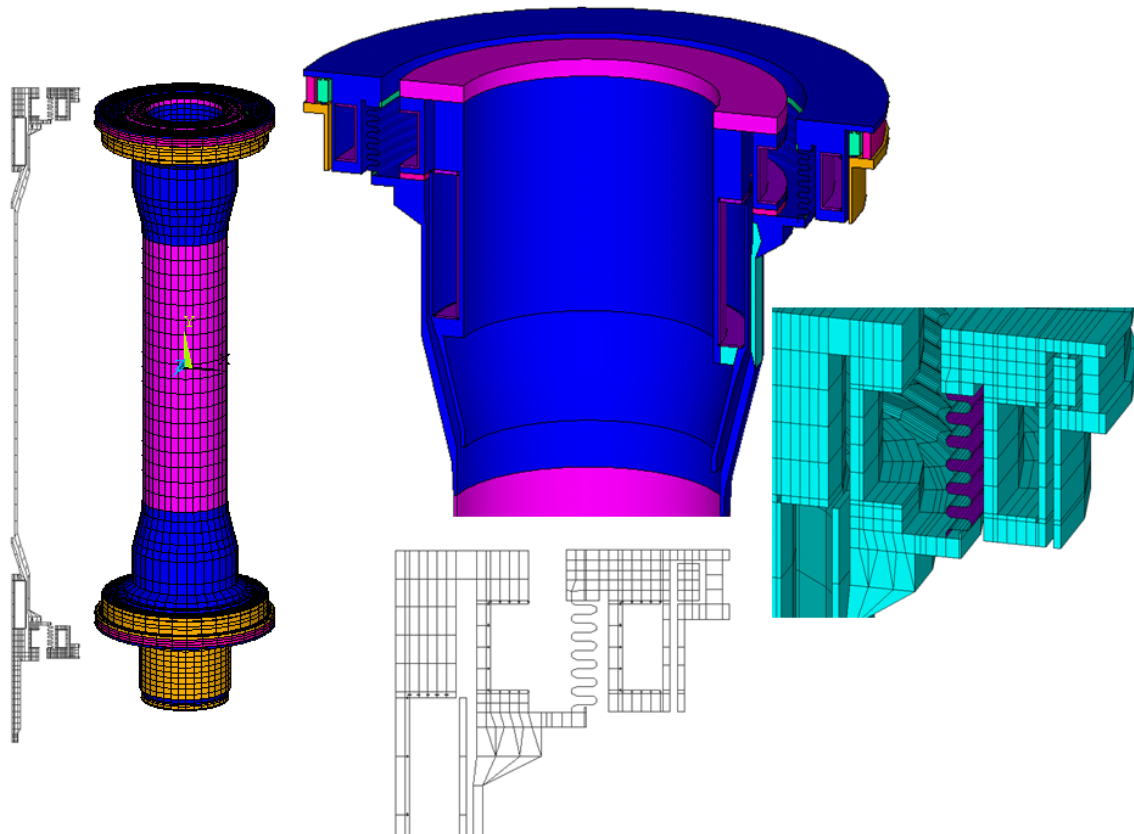


Figure 6.0-2 Swept Mesh Model of the Centerstack Casing

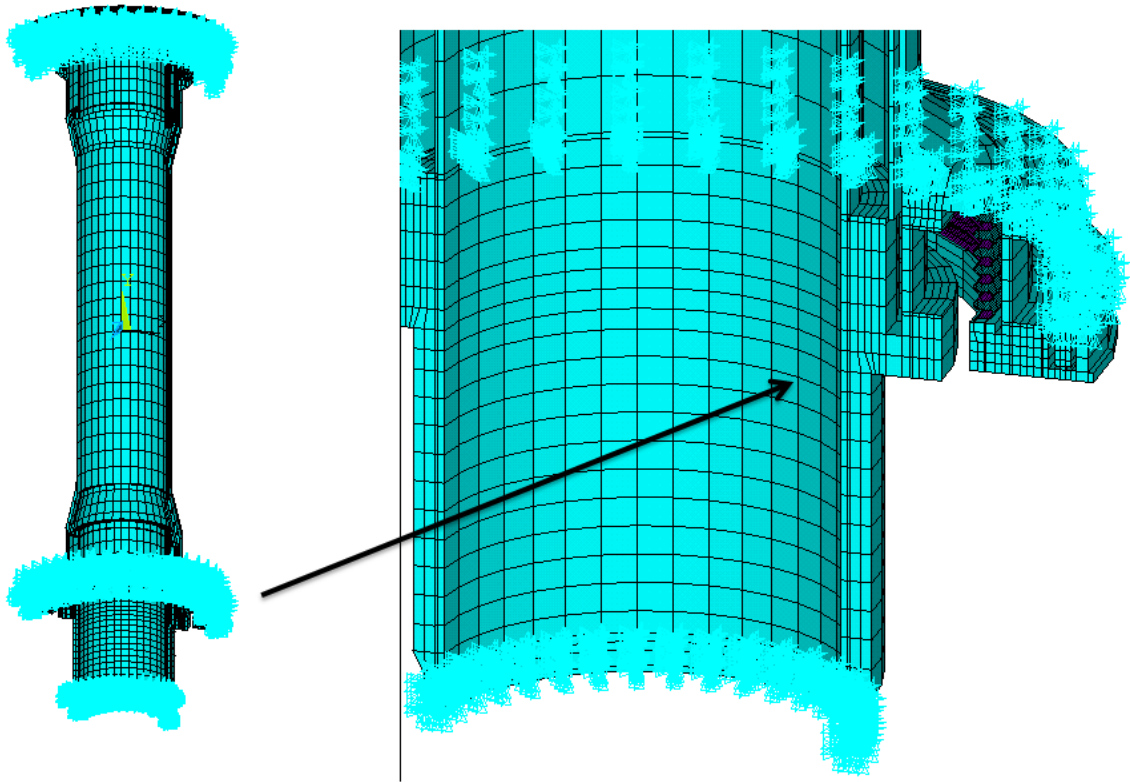


Figure 6.0-3 Swept Mesh Model of the Centerstack Casing Showing Displacement Constraints

7.0 Pressure Loading

7.1 Normal Operating Vacuum Loading

Normal operating pressures on the casing come from atmospheric pressure on the inside of the casing and produces hoop tension. The Tresca stress from this loading is 6.3 MPa.

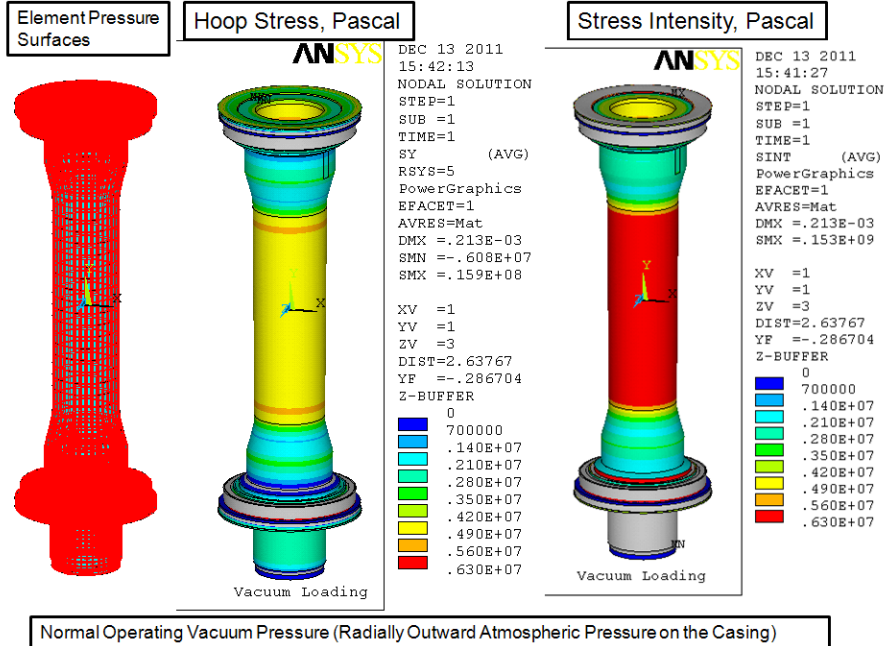


Figure 7.1.1 Operating Vacuum Load Pressure Surfaces, Hoop, and Tresca Stress

7.2 Test Vacuum Loading and Buckling

During final manufacturing tests, leak tests may be performed by closing off the top and bottom flanges and drawing a vacuum on the casing. Helium is "sprayed" on the outside welds and a mass spectrometer is used at the vacuum pumping duct. The casing must be stable with an atmosphere of external pressure. This is the opposite loading experienced during normal operation.

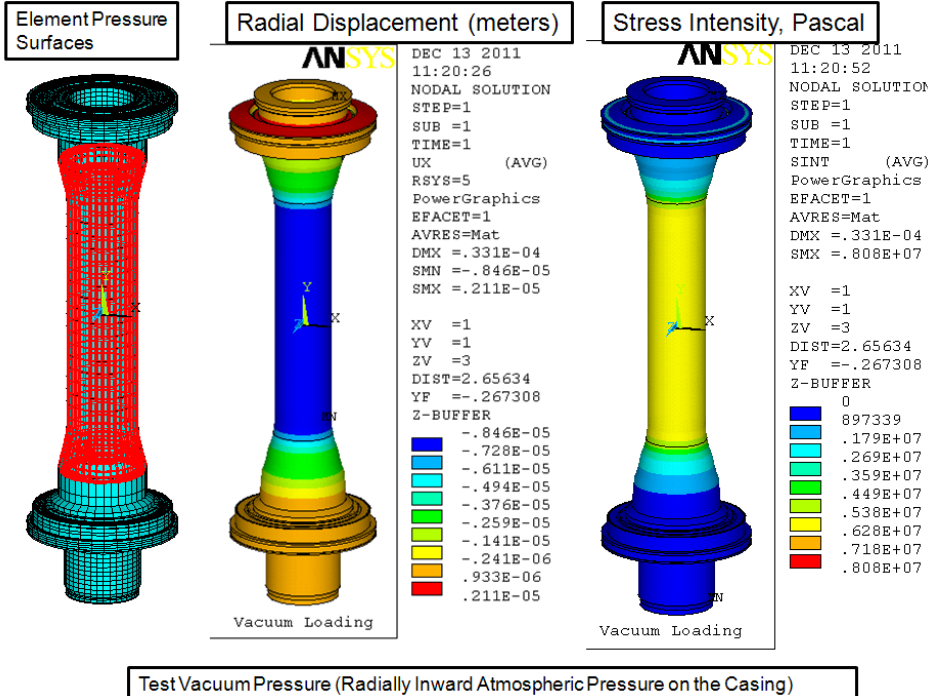


Figure 7.2-1 Test Vacuum Load Pressure Surfaces, Displacements, and Stress

Shell stresses are small during the test vacuum.

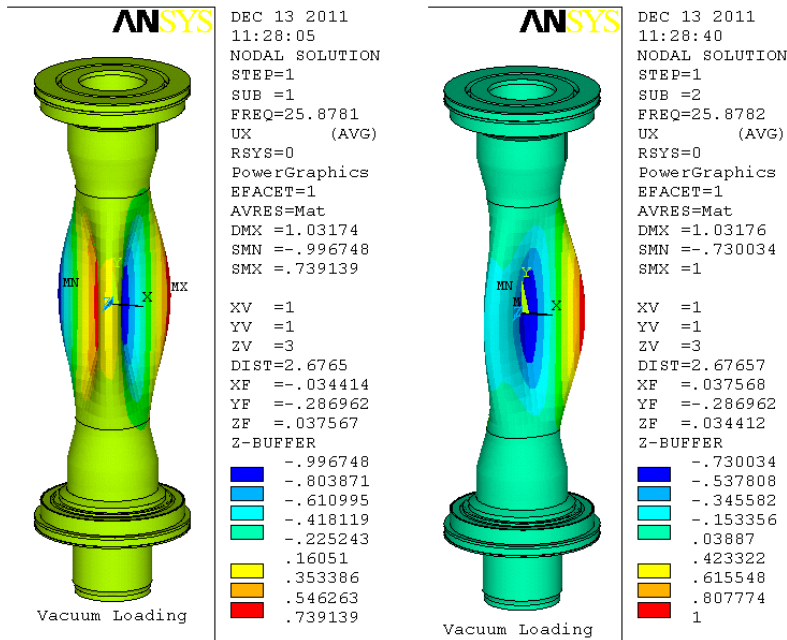


Figure 7.2-2 Buckling Modes 1 and 2

The margin against buckling for this eigenvalue buckling calculation is 25.8; well beyond the factor of 5 required in the NSTX Structural Criteria Document.

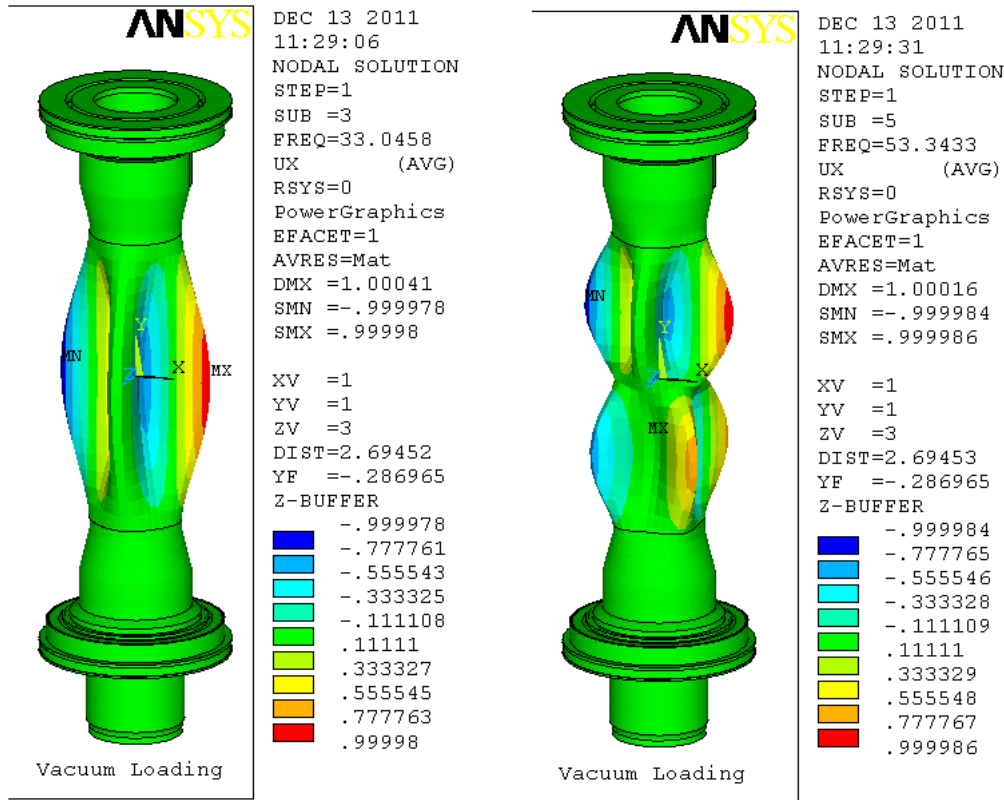


Figure 7.2-3 Buckling Modes 3 and 5

The first two modes are the most critical. Beyond this the buckling margin goes up beyond 33.

8.0 Heat Balance Results

These results are reproduced from Art Brooks' heat balance calculation, ref [3].

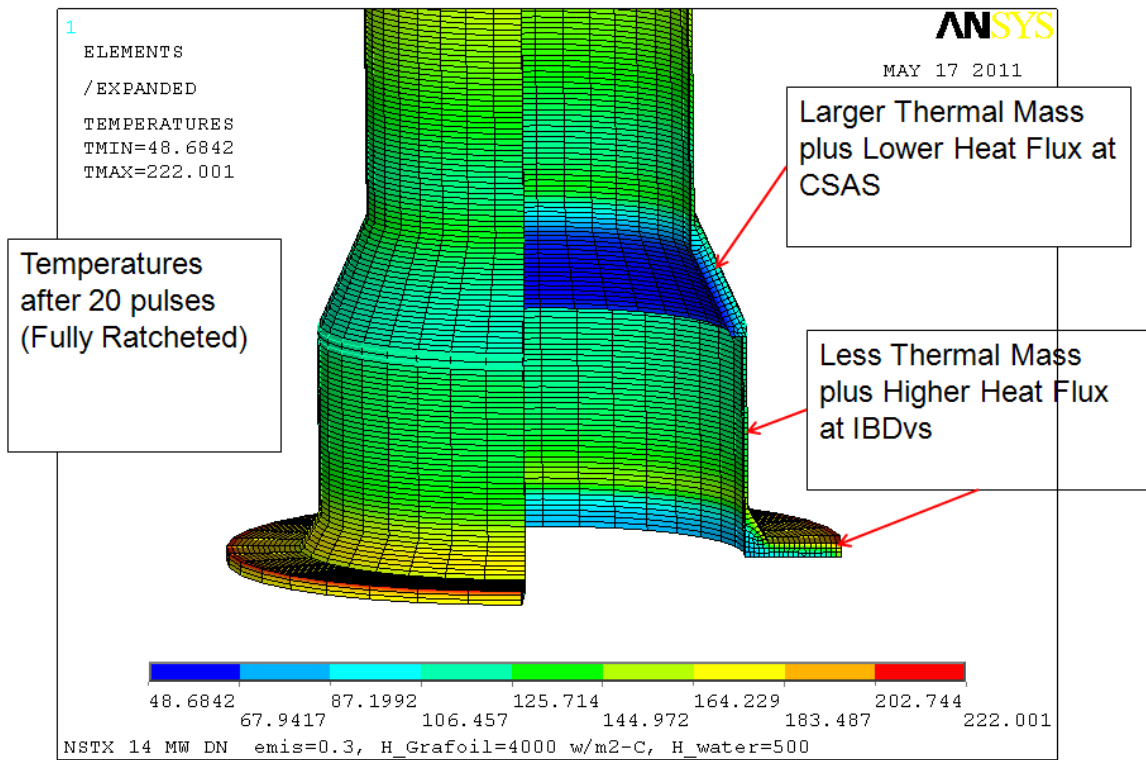


Figure 8.0-1 Temperature Distribution from the Heat Balance Calculation [3]

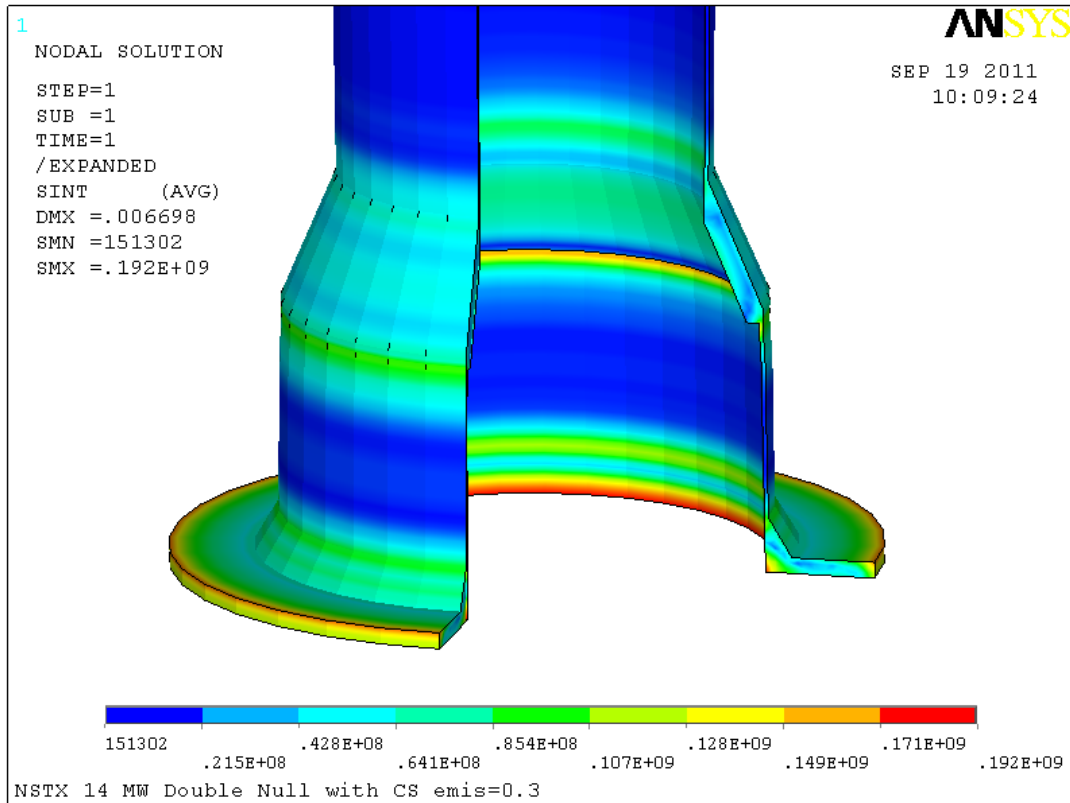


Figure 8.0-2 Temperature Stress Distribution from the Heat Balance Calculation [3]

9.0 Halo Current Results

9.1 Halo Currents in the Casing

These results are reproduced from Art Brooks' Vessel and Internals Heat Balance Calculation, ref [4].

The Tall Narrow Centerstack Could Experience Excessive Lateral Loads If Peaking Factors are Sustained.

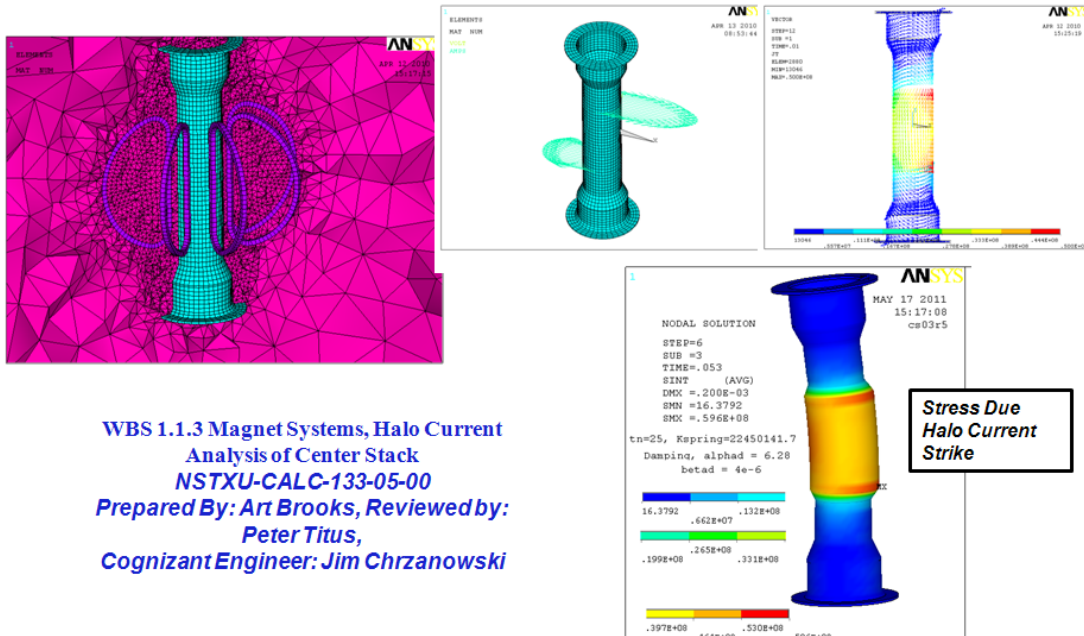


Figure 9.1-1 Halo Disruption Stress Results from [4], presented at the FDR

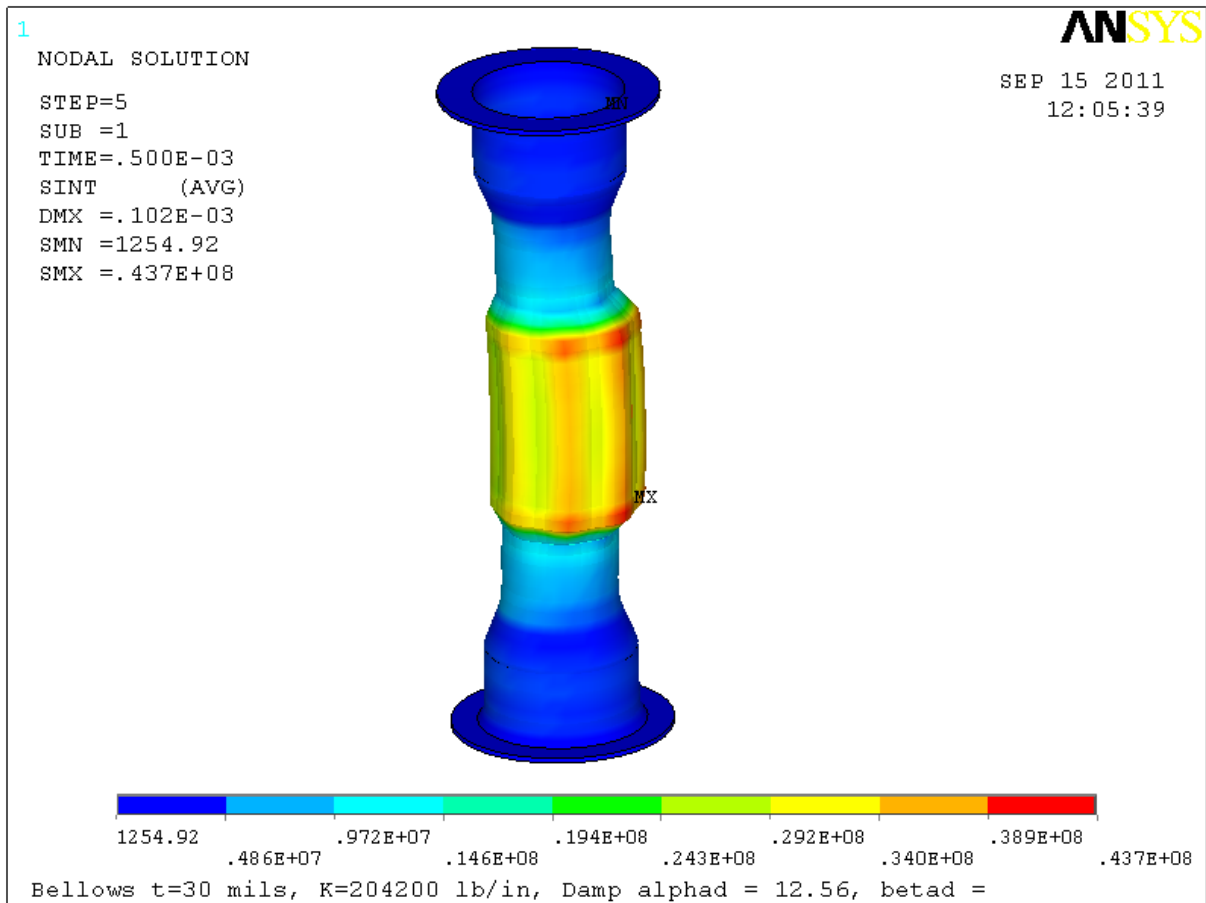


Figure 9.1-2 Halo Disruption Stress Results from [4]

9.2 Normal Operation and Halo Currents in the CHI Bus Connection

Currents flow in the CHI system during start-up and during a disruption. Normal operation for the upgrade is expected to utilize 27 kA of current [21] when the TF is at full field. This is planned to produce 1 MA of plasma current. This occurs during start-up. The CHI can be used for current drive after the initiation. This was done early in the NSTX program to demonstrate current drive but is not commonly used.

NSTX-U has the Potential for 1 MA CHI Start-up

From [21] Progress on CHI and MGI Experiments on NSTX R. Raman, et al.

CHI Start-up Parameters in NSTX and NSTX-U

Parameters	NSTX	NSTX-U
R/a (m)	0.86 / 0.68	0.93 / 0.62
Toroidal Field (T)	0.55	1.0
Planned Non-Inductive sustained Current (MA)	0.7	1.0
Poloidal flux (mWb) contained in the plasma at non-inductive sustained current with internal inductance of 0.35 and at device major radius	132	206
Maximum available injector flux (mWb)	80	340
Maximum startup current potential (MA)	0.4	~1
Req. Injector current for max. current potential (kA)	10	27*

* HIT-II routinely operated with 30kA injector current without impurity issues

FY 11 Results R. Raman, O. Mueller, T.R. Jarboe et al. Phys. Plasmas 18, 092504 (2011)

NSTX E3rd APS-OPP Raman Nov 17, 2011 14

Figure 9.2-1 Normal Operational Parameters Expected for NSTX Upgrade [21]

CHI Operation and Halo Current Path Through the CHI Connections

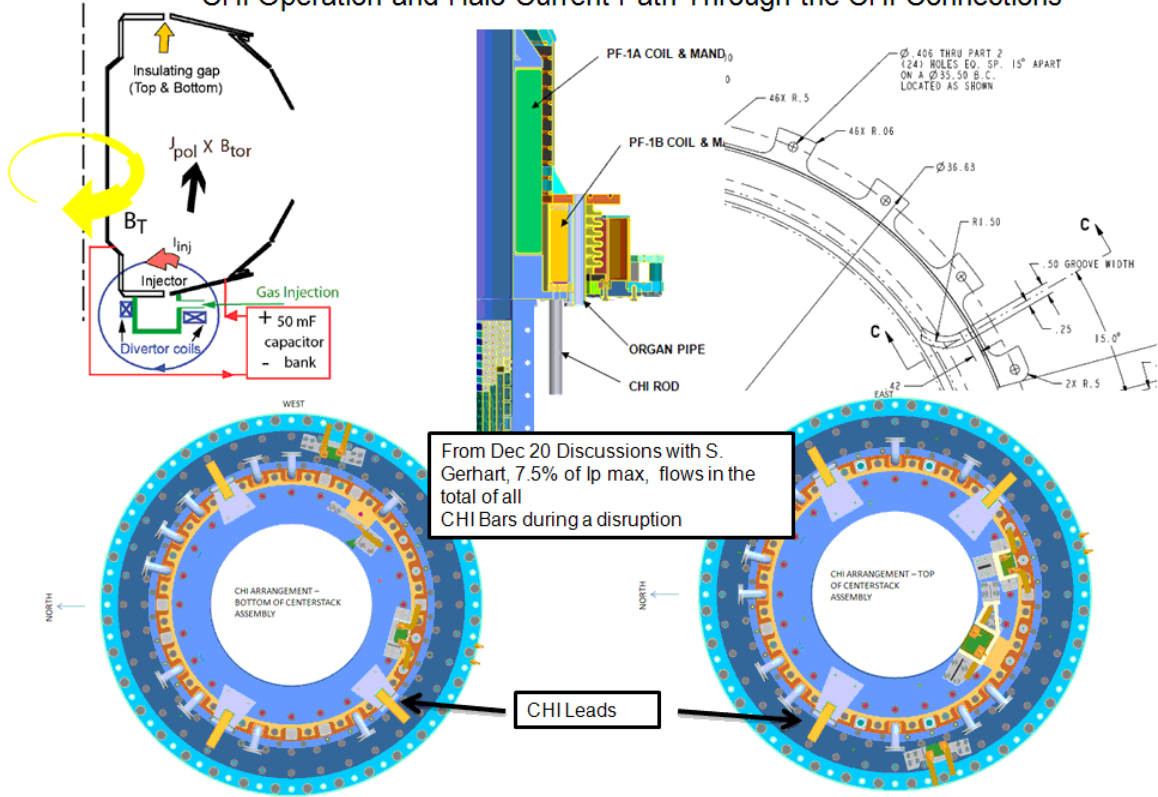


Figure 9.2-2 Layouts and Arrangement of the CHI Connections

		NSTX BASE	NSTX CSU
Ro	m	0.854	0.934
A_100		1.3	1.5
I _p	MA	1.0	2.0
B _{t@Ro}	T	0.6	1.0
I = 5e6*radius*B _t at Radius	Amp	2.562e6	4.67e6
I per Turn =	Amp	71166	129722

The toroidal field at the CHI Rod is $.934 * 1.0 / (18.31 / 39.36) = 2.008T$. Normal operating current in the CHI rods is $27 \text{ kA} / 3 = 9 \text{ kA}$. The load in the rod over almost a meter of height is $9000 * 2T = 18000N$ or 2023 lbs per rod, radially outward. The Halo loading is 7% of $2e6 \text{ amps} * 2T * 1m / 3 = 93333N = 20981 \text{ lbs}$ per rod. One important observation is that the disruption considered in Art Brooks' simulation is a centered disruption. The disruption that drives currents in the CHI bus is a quench after a VDE. So, the loading in the CHI bus is not additive to those loads calculated by A. Brooks.

10.0 Mid Plane Disruption, Quench of P1

This was thought to be an interesting disruption case. At the mid plane, the centerstack casing is not reinforced. The only structural strength comes from the 1/4 inch shell.

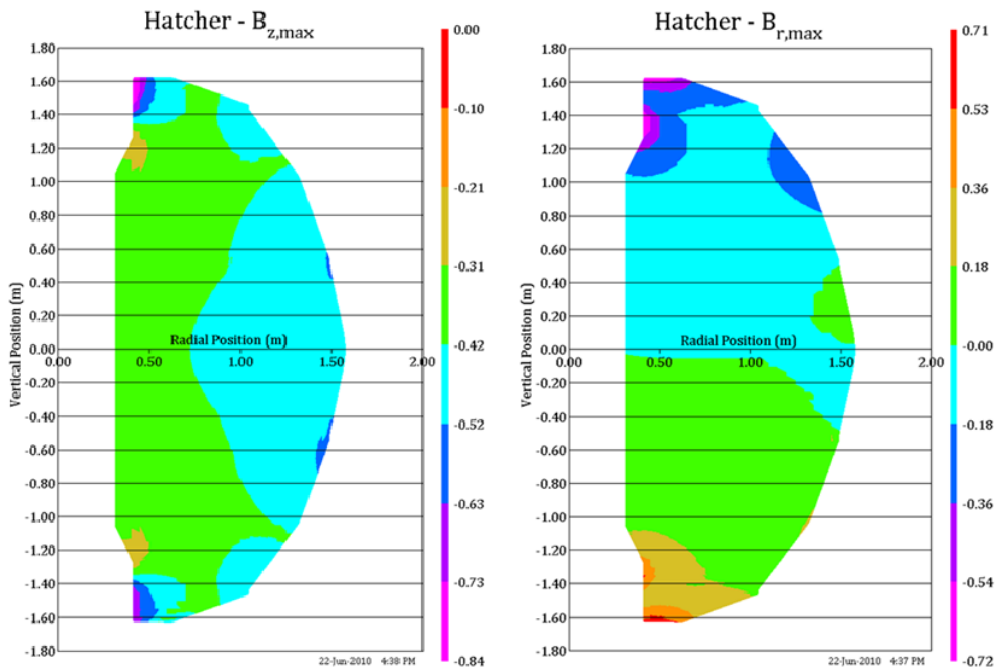


Figure 10.0-1 Max Poloidal Fields for All 96 Equilibria

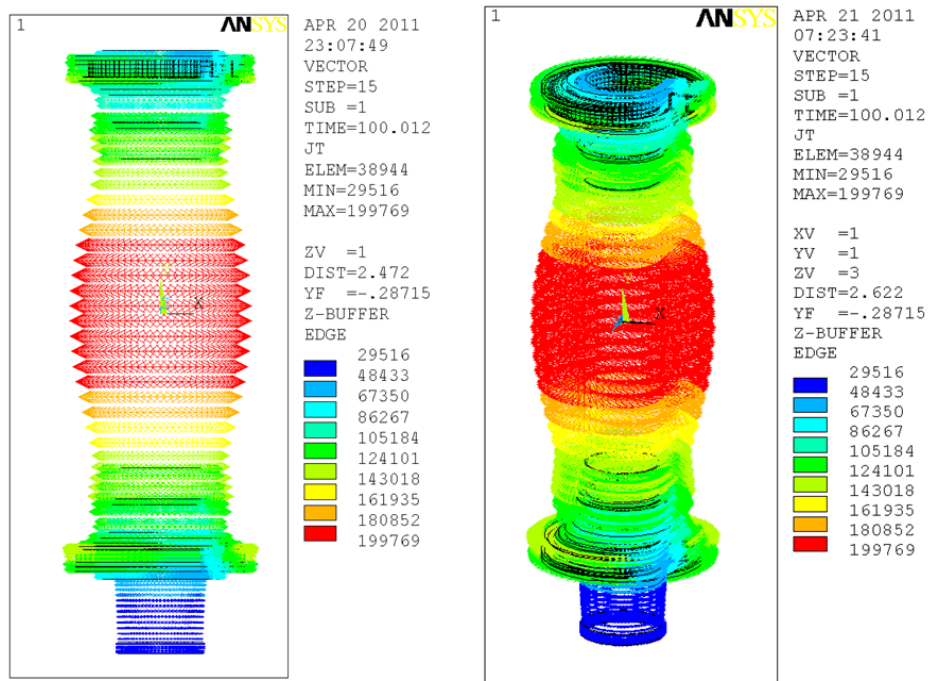


Figure 10.0-2 Current Density Vectors for the Mid-Plane Disruption

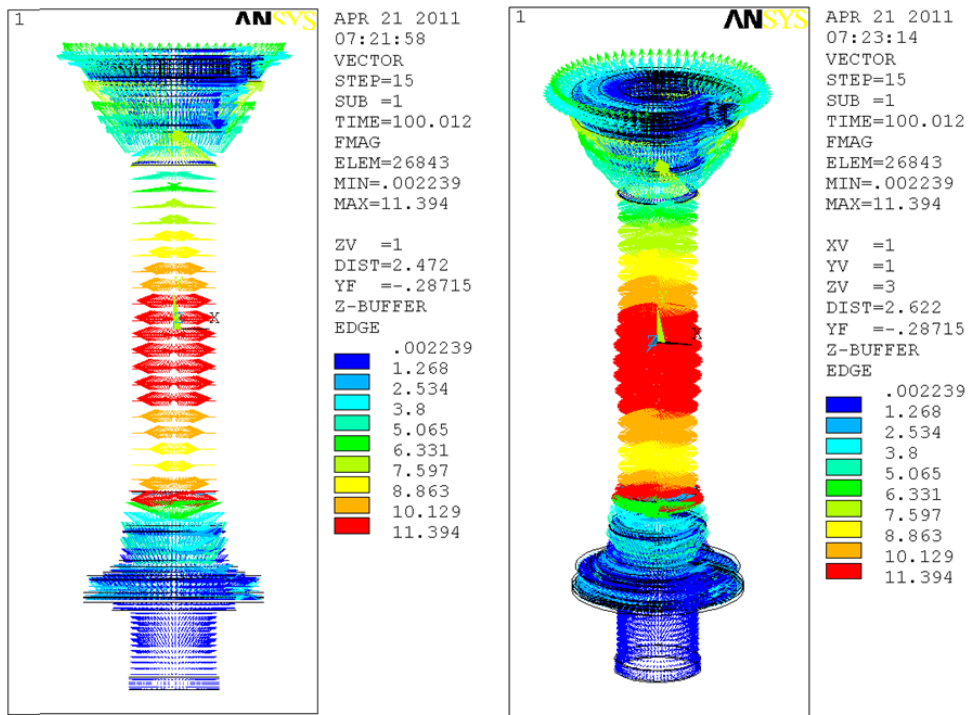


Figure 10.0-3 Lorentz Forces Resulting from Toroidal Currents (Figure 10.0-2) and the Poloidal Field (Figure 10.0-1)

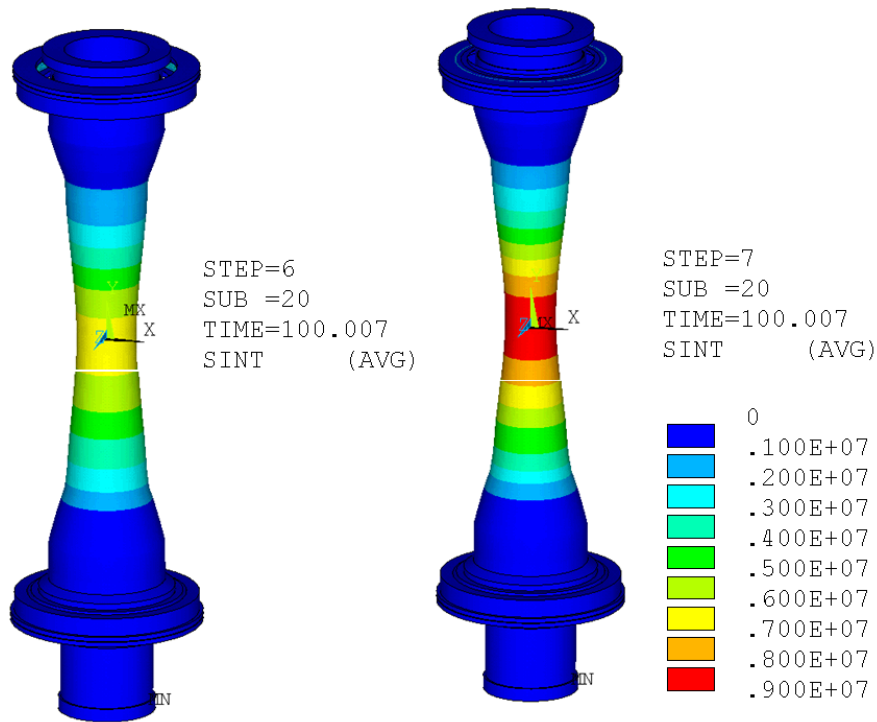


Figure 10.0-4 Dynamic Casing Stresses for the Worst Time Point (100.007) in the Disruption. See Time History Plot in Figure 10.0-5

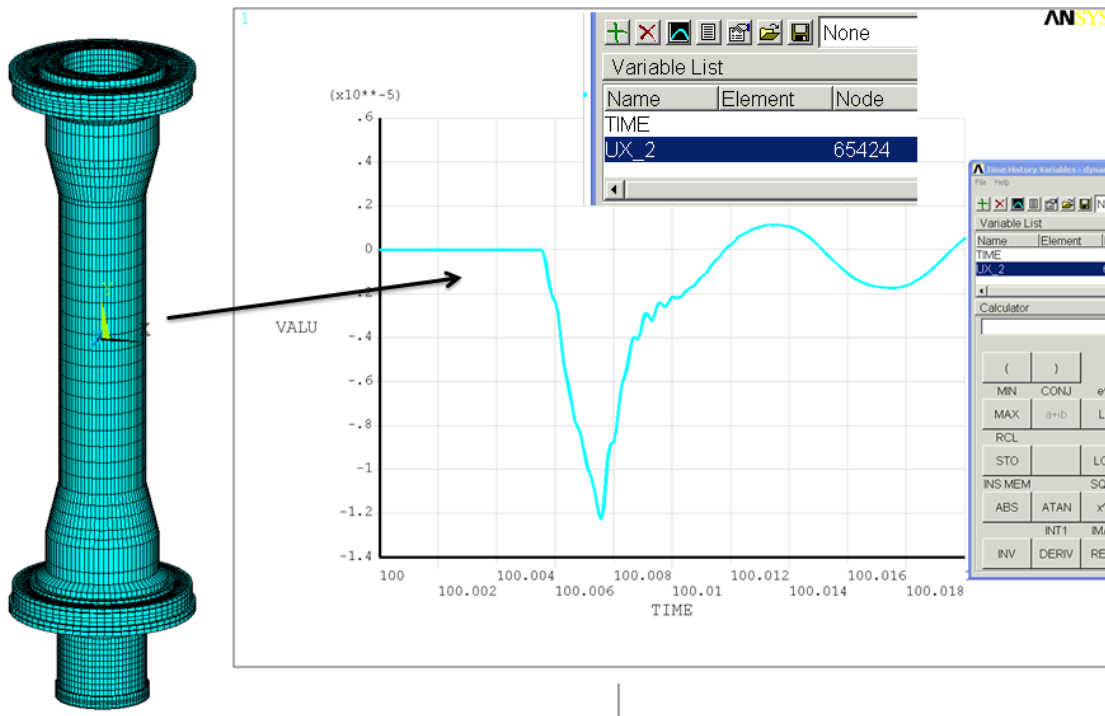


Figure 10.0-5 Dynamic Time History Response of the Casing showing the largest deflection occurring at 100.007 seconds.

11.0 Translations and VDE's

11.1 Slow Mid Plane Translation and Quench P1 to P2

Reference [10] includes the mid plane translation and quench. The results are presented in this section. As for the previous mid-plane disruption, the stresses are small.

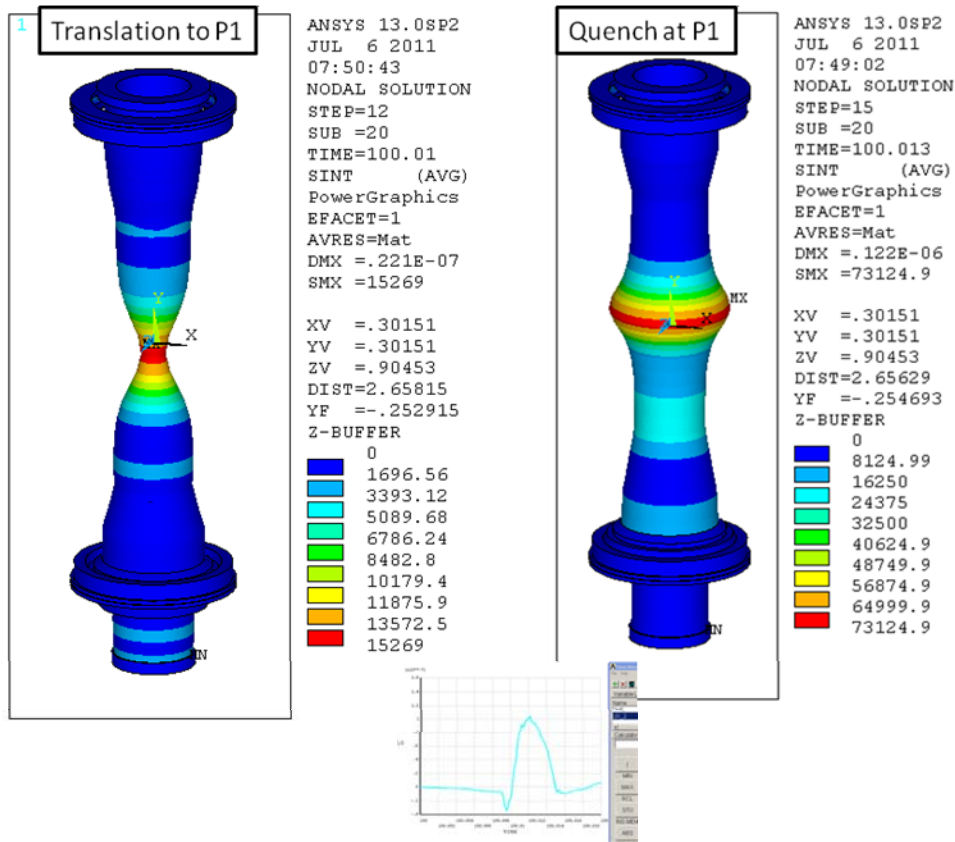


Figure 11.1-1 CS Casing Stresses for Translation and Quench

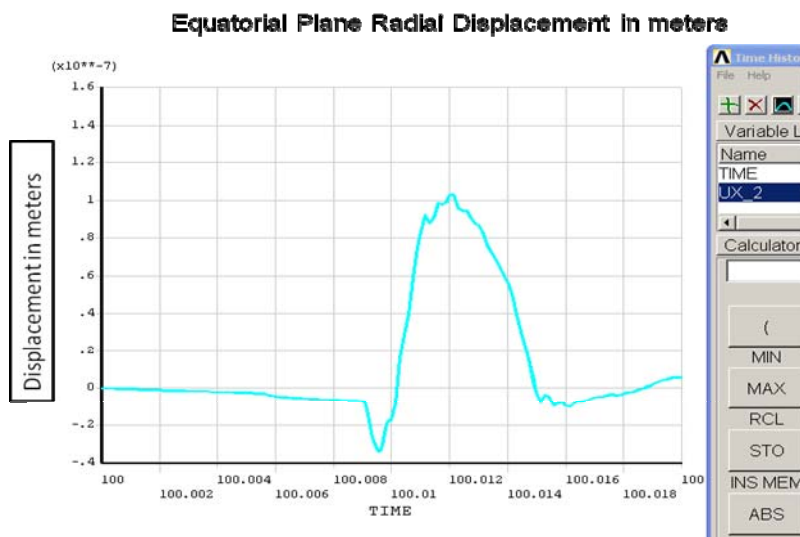
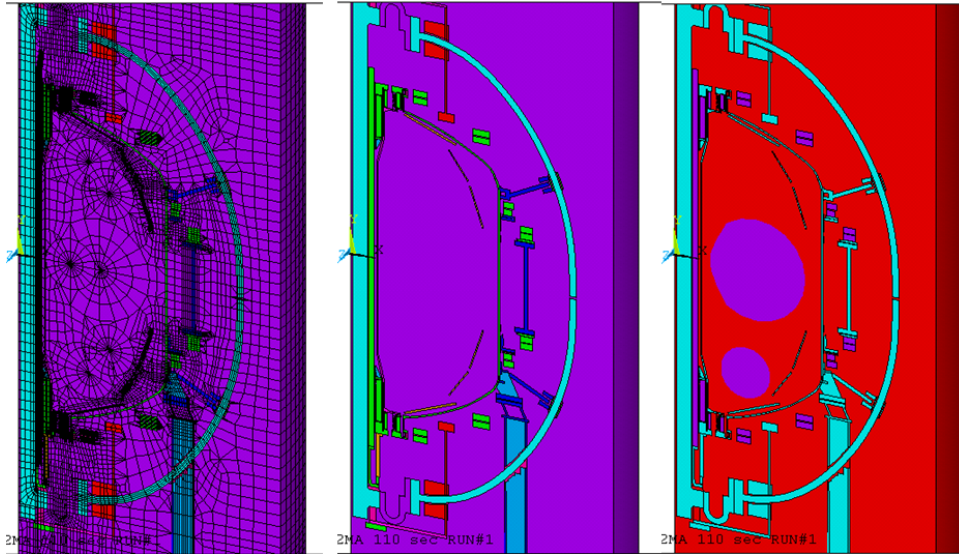


Figure 11.0-2 CS Casing Equatorial Plane Radial Displacement Post 26 Time History

11.2 P1 to P5 10 ms VDE Fast Quench at P5

Appendix I of reference [10] introduces another disruption simulation. Simulation of the passive plate disruptions also includes other structures including the centerstack casing.



Mesh, Including Air Materials Solid 97 Type
Figure 11.2-1 Appendix I of Reference 10 Electromagnetic model

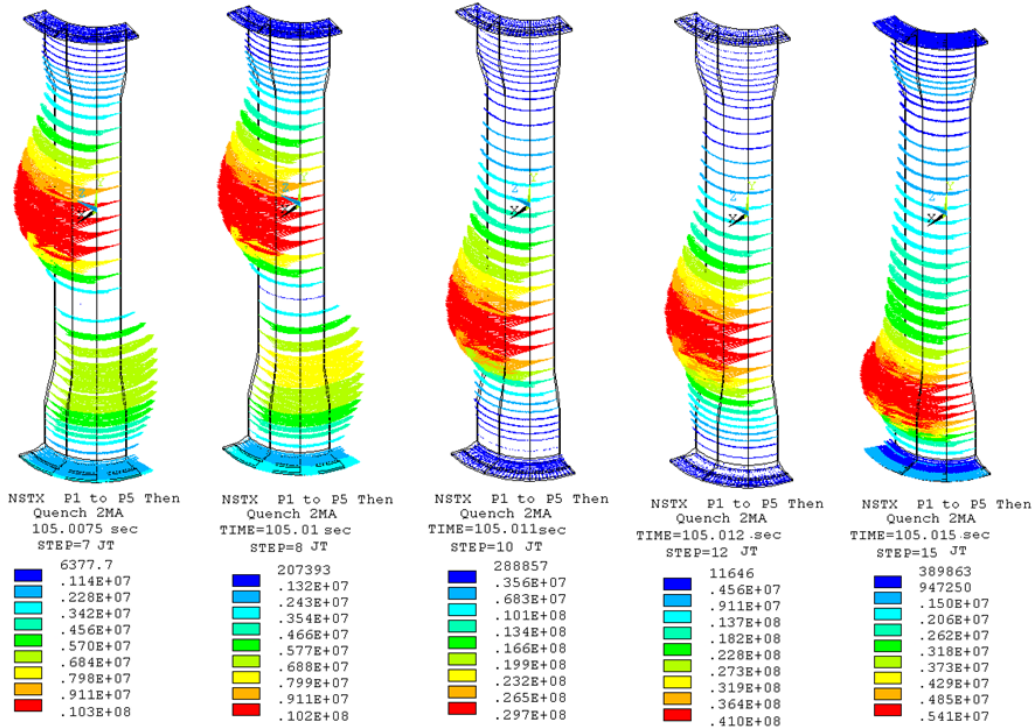


Figure 11.2-2 Current Densities, P1-P5, 10ms VDE (ends at Step 8) and Quench at P5

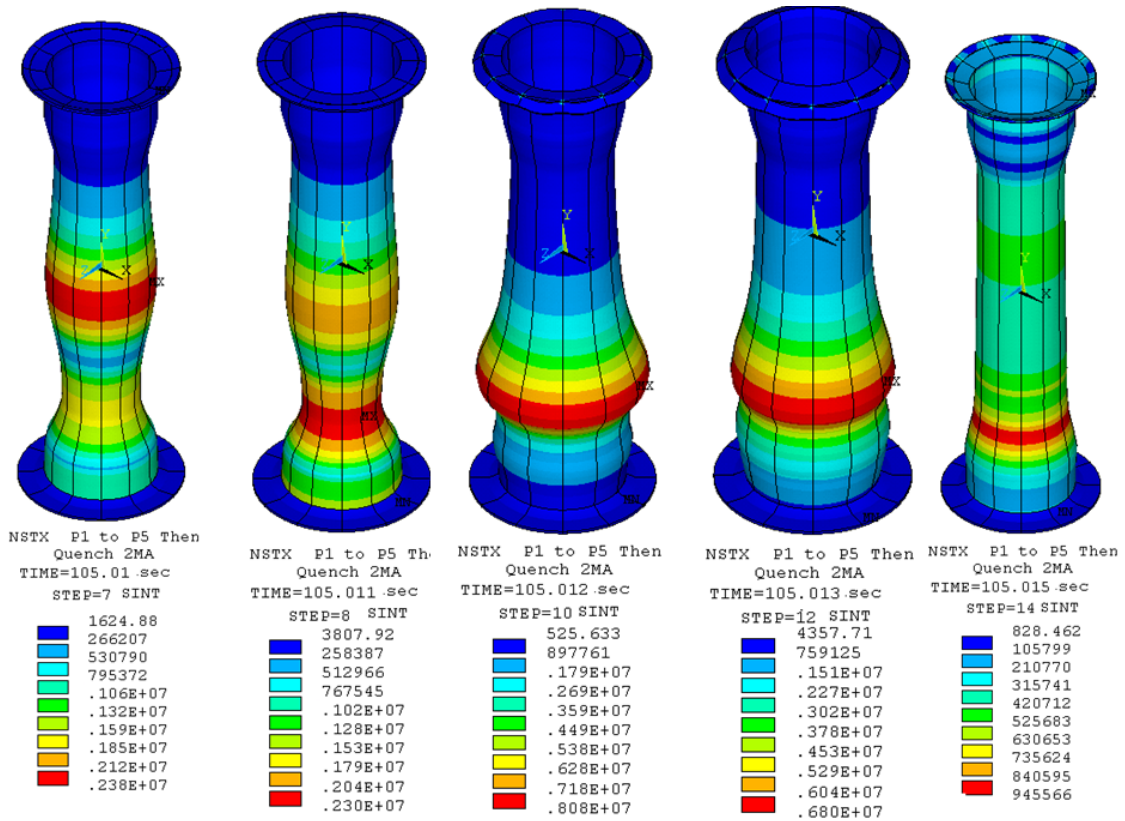


Figure 11.2-2 Tresca Stress, P1-P5, 10ms VDE (ends at step 8) and Quench at P5
 This Disruption Simulation produces nothing more than 8.08 MPa.

12.0 Tile Moments

The tile eddy currents will produce net moments about the vertical axis and net to zero moment radially.

- **Tile layout**

- Reduced overall tile number, increased size where possible

- ~900 → ~700 tiles
 - IBD HS Tiles kept the same size due to thermal constraints

- Designed diagnostic slots and wire channels

- Mirnov, Rogowski, Langmuir, Thermocouple

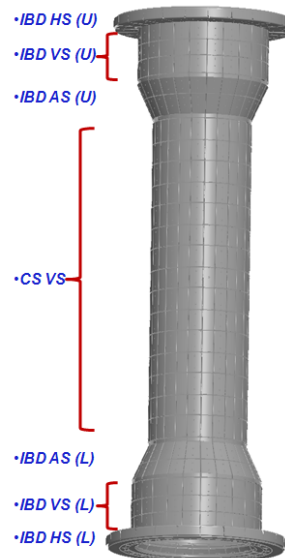
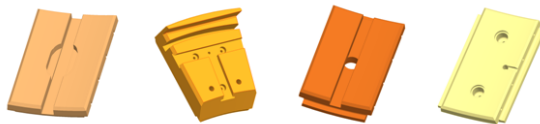


Figure 12.0-1 Tile Inventory from Kelsey Tresemer's FDR Presentation

From Ref [16]:

CSFW Tiles

There are two types of CSFW tiles: fixed tiles and floating tiles. The fixed tiles are held in place vertically and radially by four pins that run through the entire tile horizontally. Horizontally, they are held by a mounting bracket as well as two locating pins. However, the locating pins have a large tolerance and are unlikely to be a real constraint.

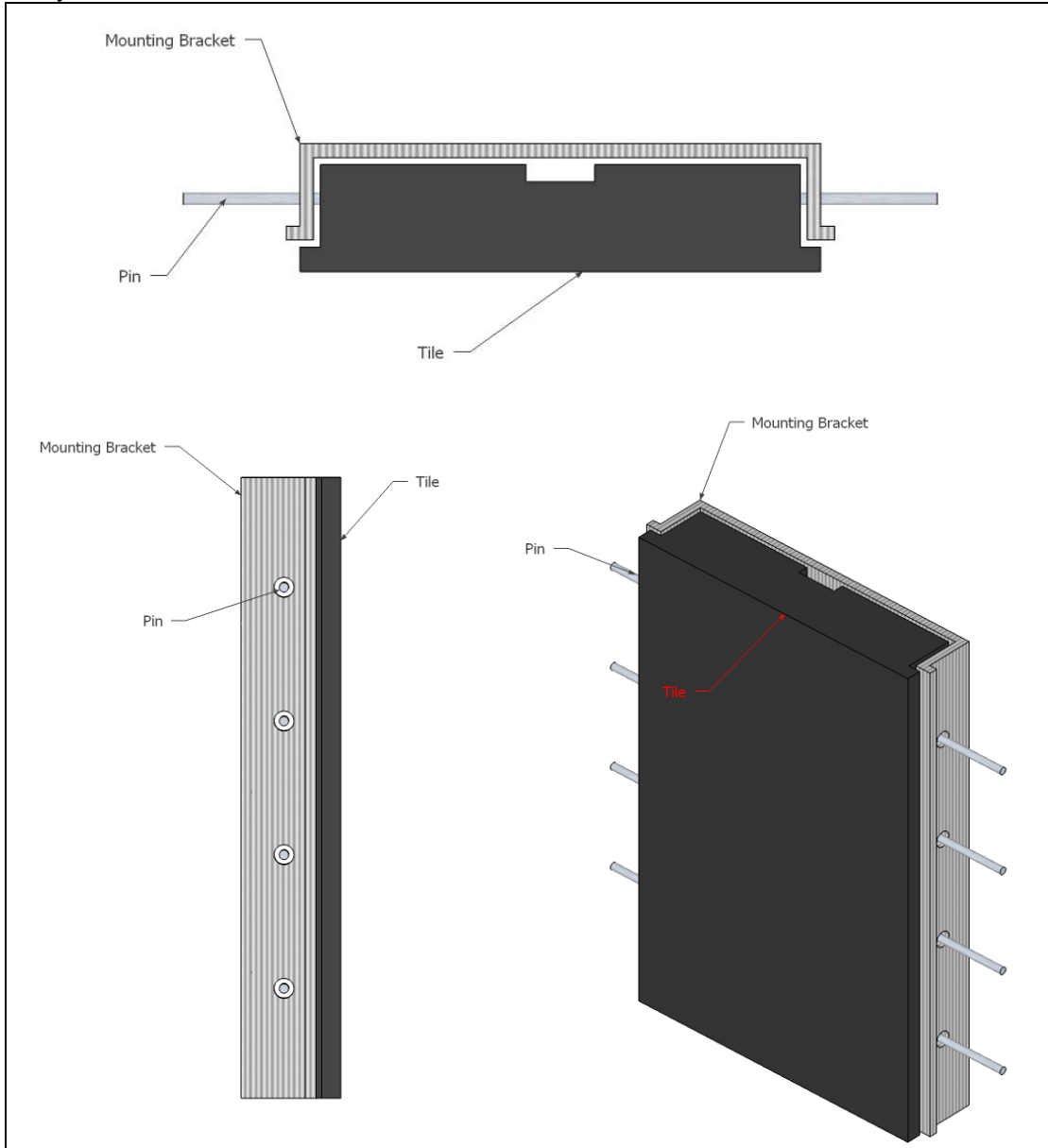


Figure 1. Top, side, and isometric views of the fixed CSFW tile.

The images above are simplified models of the tile. These images are not to scale and are used only as similar geometries. The mounting bracket is screwed into the centerstack using bolts that are behind the tile and are tightened through small holes in the surface of the tiles.

The CSFW floating tiles are similar to the fixed tiles in shape. However, they are freer to translate. The tiles are held radially and vertically by the ends of the pins that hold the fixed tiles in place. Horizontally, they are held by fixed tiles on either side. The fixed and floating tiles are placed in an alternating pattern to allow this mounting method. For both the fixed and floating tiles, the following dimensions, loads, or parameters were used in the ANSYS qualification script.

Variable Name	Value	Units
Material	7 (Thermagard)	None
Tile width	3.4	inches
Tile height	5.8	inches
Tile thickness	0.75	inches
T1	0.5	inches
T2	0.5	inches
T3	0.0625	inches
T4	0.0625	inches
Heat flux	0.13×10^6	W/m ²
B across face horizontally	0	T/s
B across face vertically	590	T/s
B normal to face	160	T/s
B field across face horizontally	2.97	Tesla
B field across face vertically	-0.37	Tesla
B field normal to face	0.07	Tesla
Halo current density across face horizontally	0	A/m ²
Halo current density across face vertically	7.76×10^6	A/m ²
Halo current density normal to face	2×10^6	A/m ²

From Art Brooks Tile Moment Estimator:
Based on linear scaling of SPARK model results

Note: Yellow Fields for Inputs

Time Constant

Width(in)		3.4	in
Height(in)		5.8	in
radius	r	0.063637372	m
diameter	d	0.127274744	m
thickness	t	0.01905	m
resitivity	rho	1.17E-05	ohm-m
time constant	tau	2.47E-05	s

Equivalent radius

ATJ Graphite

Field Change

Inductive	dB	0.59	T
Ramp Time	dt	0.001	s
Resistive	dBdt	590	T/s

Note: Inductive for dt << tau, Resistive for dt >> tau

Induced current

Inductive	I_ind	37546.0494	amps
Resistive	I_res	973	amps
	I_ind*EXP(-dt/tau)	0	amps
	I_res*(1-EXP(-dt/tau))	973	amps

Note: Linear Scaling From SPARK Analysis

Note: Linear Scaling From SPARK Analysis

Forces and Moments

Dipole Current	I_dp	973	amps
Dipole area	a	0.012722555	m ²
Dipole Moment	m	12.37371058	amps-m ²
		2888.56443	m ²

Over estimate for resistive solution, reasonable for inductive

Field	Btf	2.97	T
	Bpf	0.37	T

Torque = mxB	Mpol	36.75	N-m	325	in-lbs
	Mtor	4.58	N-m	41	in-lbs

27 ft-lbs
3 ft-lbs

Dipole moment is normal to tile
Torques are about poloidal and toroidal axes thru tile

The central sleeve of the casing is 89 inches long and 23 inches in diameter. The number of tiles on this section of the casing is $89 \times 23.29 \times 3.1416 / 3.4 / 5.8 = 330$ tiles. The net moment acting on the thin part of the casing is $27 \times 330 \times 12 = 106,920$. The moment will be reacted by the lower flanges and the upper and lower bellows. The moment will be split between the upper and lower ends of the shell. The shear stress is then $106,920 \text{ in-lbs} / 23.29 / \pi / .25 / 2 = 2922.6 \text{ psi}$ (20.15 MPa) shear. Tresca stress is 40.3 MPa. At the top and bottom flanges, torques from all 700 tiles must be reacted. Assuming that all the tiles are similar to the CSFW tiles, the total moment is $27 \times 700 \times 12 = 226,800 \text{ in-lbs}$. This is reacted in the heavier cylindrical sections at each end of the casing. These are 30 inches in diameter and 0.438 inches thick. The torsional shear is then $226800 / 2 / 30 / \pi / .438 = 2747 \text{ psi} = 19 \text{ MPa}$ Shear or 38 MPa Tresca.

13.0 PF Loading Results

13.1 Stress Results from Ref [2]

- The 2D model identifies EQ31 (PF_Currents_Forces) as producing the max vertical tensile stress in the structure, as PF1a/b upper and PF1a/b lower pull away from the mid-plane with 56 kip.
- In this top-half symmetry model, 12.7 and 43.3 kip are applied to the PF1a and PF1b upper flanges, respectively.

Notice that the max stress of 45 MPa also appears in the center column to transition piece weld, which is comparable to the 50 MPa 2D result ($\ll 300 \text{ MPa}$)

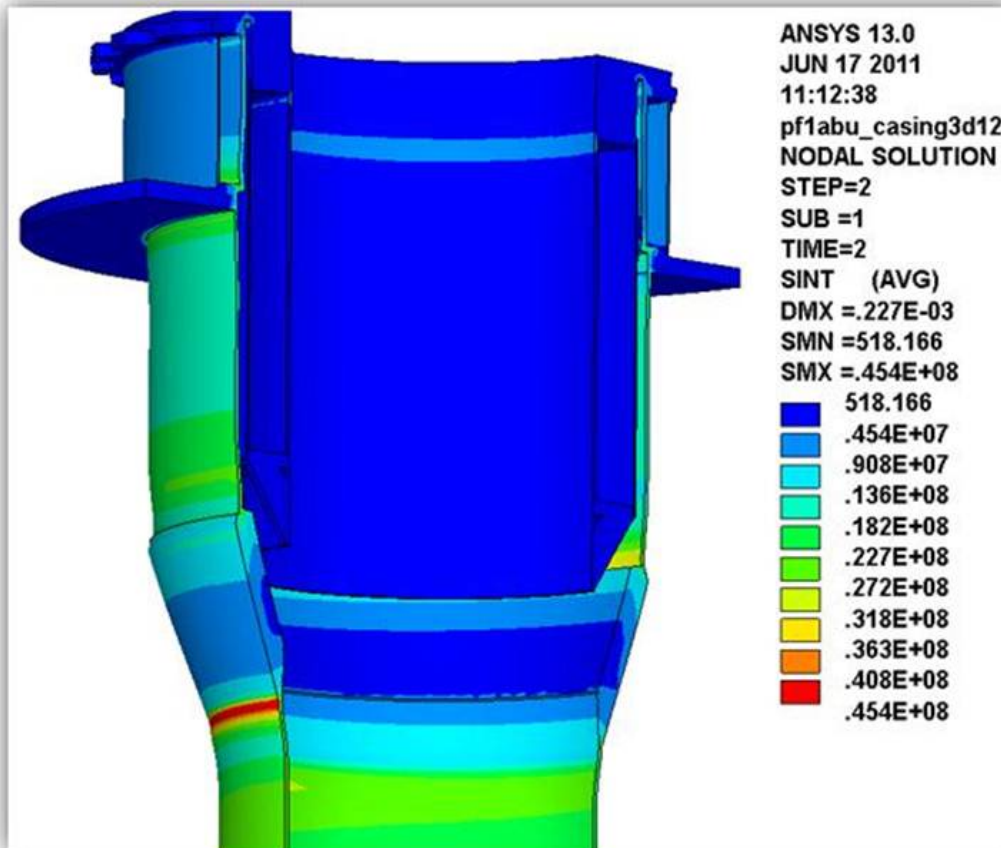


Figure 13.1-1 Stress Results from [2]

13.2 Buckling

L. Myatt did a buckling calculation based on the compressive load from the upper inner PF coils. This showed a large margin. Buckling will be aggravated by the thermal expansion of the central region of the casing, and possibly any tolerance or other geometric imperfections introduced during manufacture, assembly or operation.

Center Tube Buckling Stability

- Loads from E1 produce a compressive load in the ¼" thick central tube of 86 kip, which raises the concern over buckling.
- Roark's equation for the critical stress (σ') in thin cylindrical tubes is:
 - $\sigma' = E(t/R) / \{3^{1/2}(1-\nu^2)^{1/2}\}$
 - $\sigma' = (29\text{Msi})(0.25/11.64) / \{3^{1/2}(1-0.3^2)^{1/2}\} = 380 \text{ ksi}$
- The average stress in the central tube:
 - $\sigma_{\text{tube}} = (86 \text{ kip}) / (2\pi \cdot 11.64" \cdot 0.25") = 4.7 \text{ ksi}$
- The ratio of critical stress to max stress is ~ 80 ($\gg 5$)

Figure 13.2-1 L. Myatt's buckling calculations

L. Myatt's calculations are based on Roark handbook calculations and do not include lateral loading from magnetic misalignments or differential thermal expansion. An Eigenvalue buckling analysis of the centerstack casing was performed. The thermal expansion of the central region was approximated by selecting +/- 1 meter from the equatorial plane and applying 200 degrees C. The ANSYS instructions say that you should do a static solution first. This was done with the thermal plus Lorentz loading.

```

**** EIGENVALUES (LOAD MULTIPLIERS FOR
BUCKLING) ****
*** FROM BLOCK LANCZOS ITERATION ***

SHAPE NUMBER   LOAD MULTIPLIER

1             1.9606716
2             1.9651602
3             1.9651725
4             1.9791568
5             1.9791584
6             1.9840488
7             1.9879713
8             1.9879753
9             1.9944995
10            1.9986775

EIGENVALUES AT CURRENT LANCZOS CYCLE
1 0.19606716E+01  2 0.19651602E+01  3 0.19651725E+01
4 0.19791568E+01  5 0.19791584E+01  6 0.19840488E+01
7 0.19879713E+01  8 0.19879753E+01  9 0.19944995E+01
10 0.19986775E+01 11 0.19986867E+01 12 0.20001489E+01
13 0.20001529E+01

number of steps   : 12
eigenvalues found : 13
total no. eigenvalues: 13
1
    
```

Figure 13.2-2 Buckling Results with the Thermal Loading as a Part of the Load Vector

When ANSYS reports the load factors they are based on the full load vector in the initial static analysis. The results for the casing showed only load factors of 2 when the Euler buckling hand calculations showed factors of 50.

Lorentz Forces, No Thermal Distortions

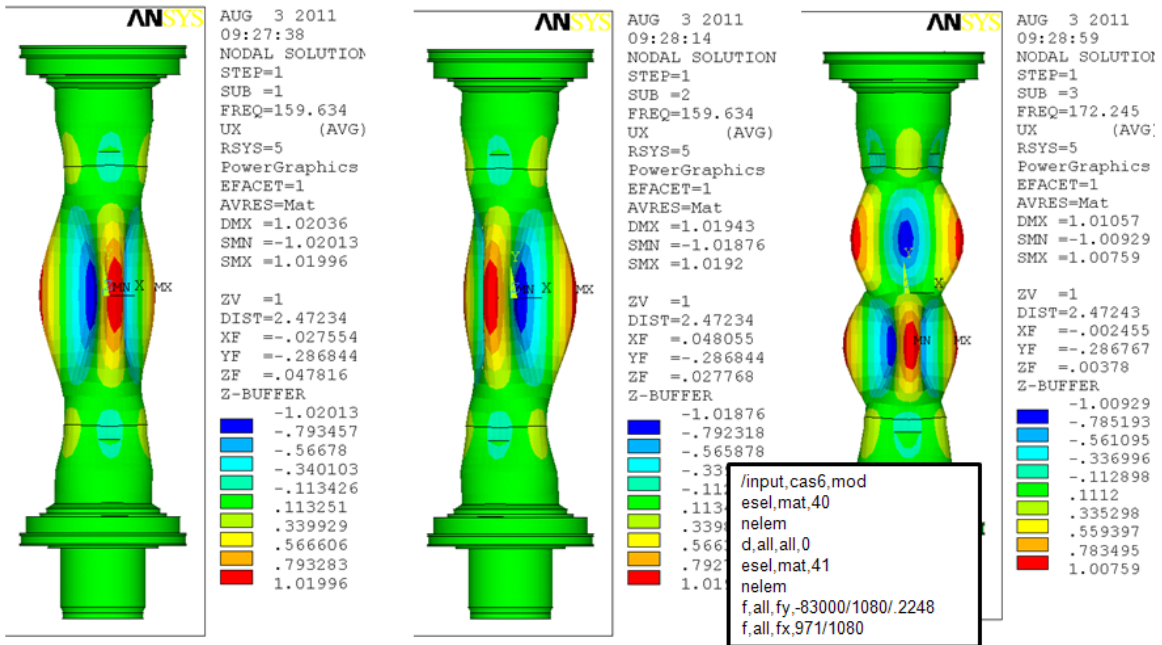


Figure 13.2-3 Eigenvalue Buckling modes and Load Factors with No Thermal Distortions

The Eigenvalue buckling was rerun without the thermal loading and the load factors went up to 160 to 170.

Lorentz Forces, With Thermal Distortion Modeled as a Geometric Alteration

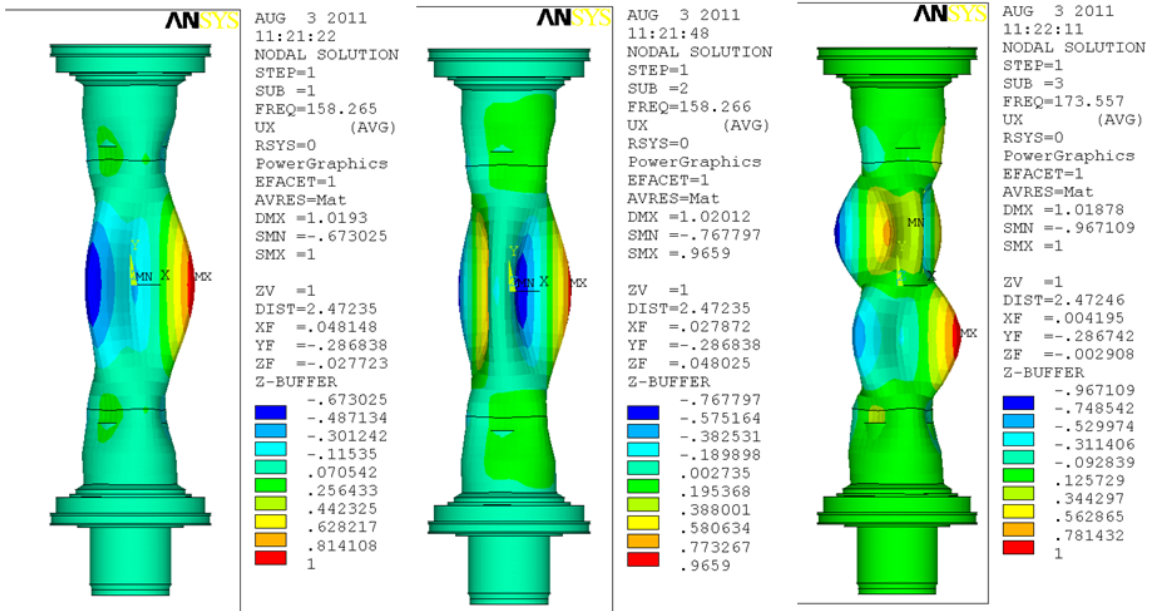


Figure 13.2-4 Eigenvalue Buckling modes and Load Factors with Thermal geometric Distortions

The thermal distortions were input with an initial geometric distortion so that the thermal effects would be considered a geometric imperfection rather than a part of the load. The load factors reduced but not by a substantial amount. The first mode factor went from 159 down to 158.

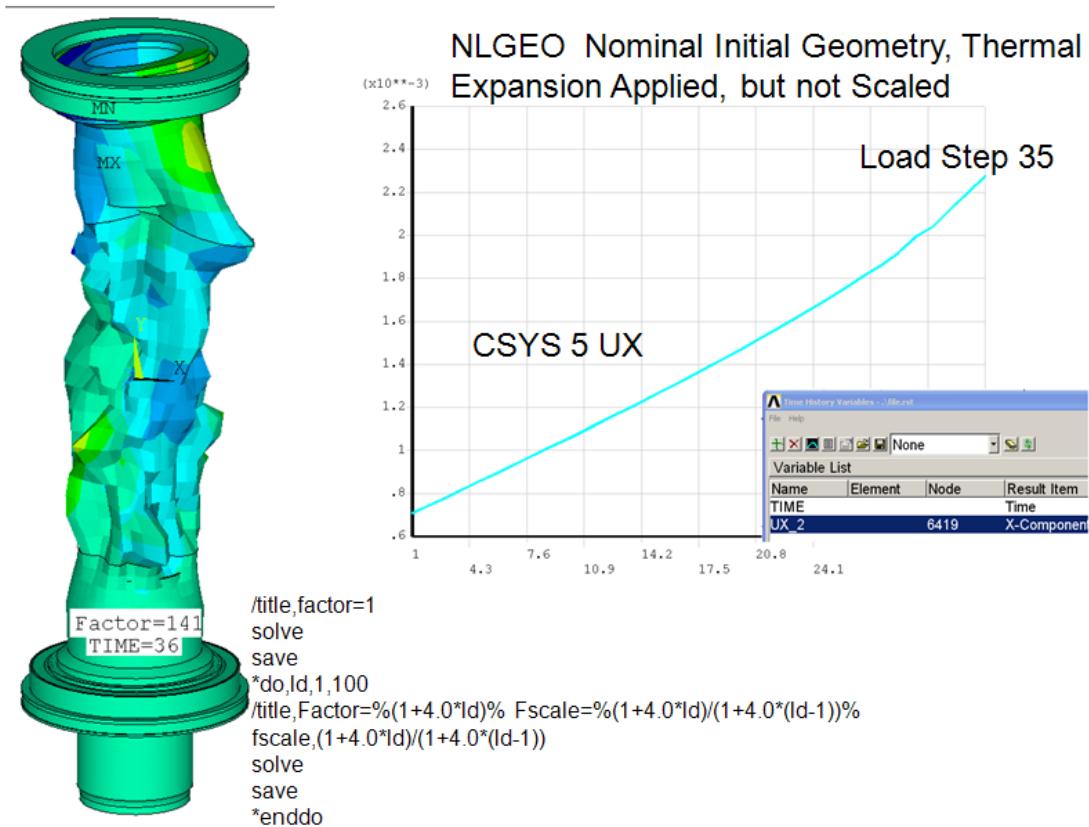


Figure 13.2-5 Non-Linear Geometry Solution - Radial Displacement as a Function of Load

The NLGEO results show factors of 141. The NLGEO analysis kept the thermal loads static and the Lorentz loads were stepped up.

NLGEO Nominal Geometry, Thermal Expansion Applied, but not Scaled, Additional Lower Half Oval by 1mm

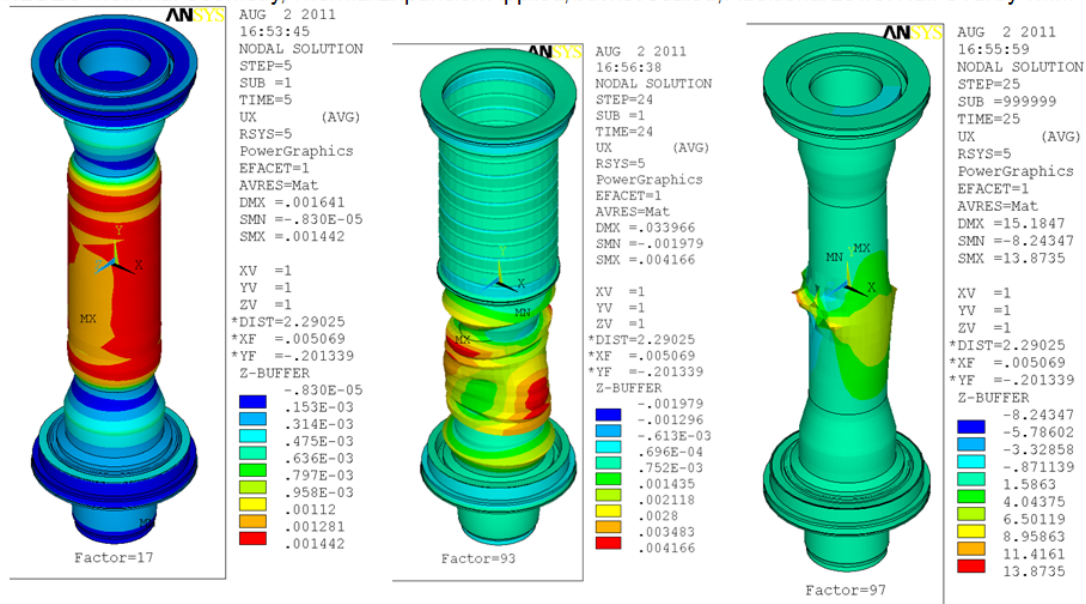


Figure 13.2-6 NLGEO Nominal Geometry, Thermal Expansion Displacement Applied, but not Scaled, Additional Lower Half Oval by 1mm (Representing Fabrication Tolerance)

14.0 Torsional Loading from TF OOP loads

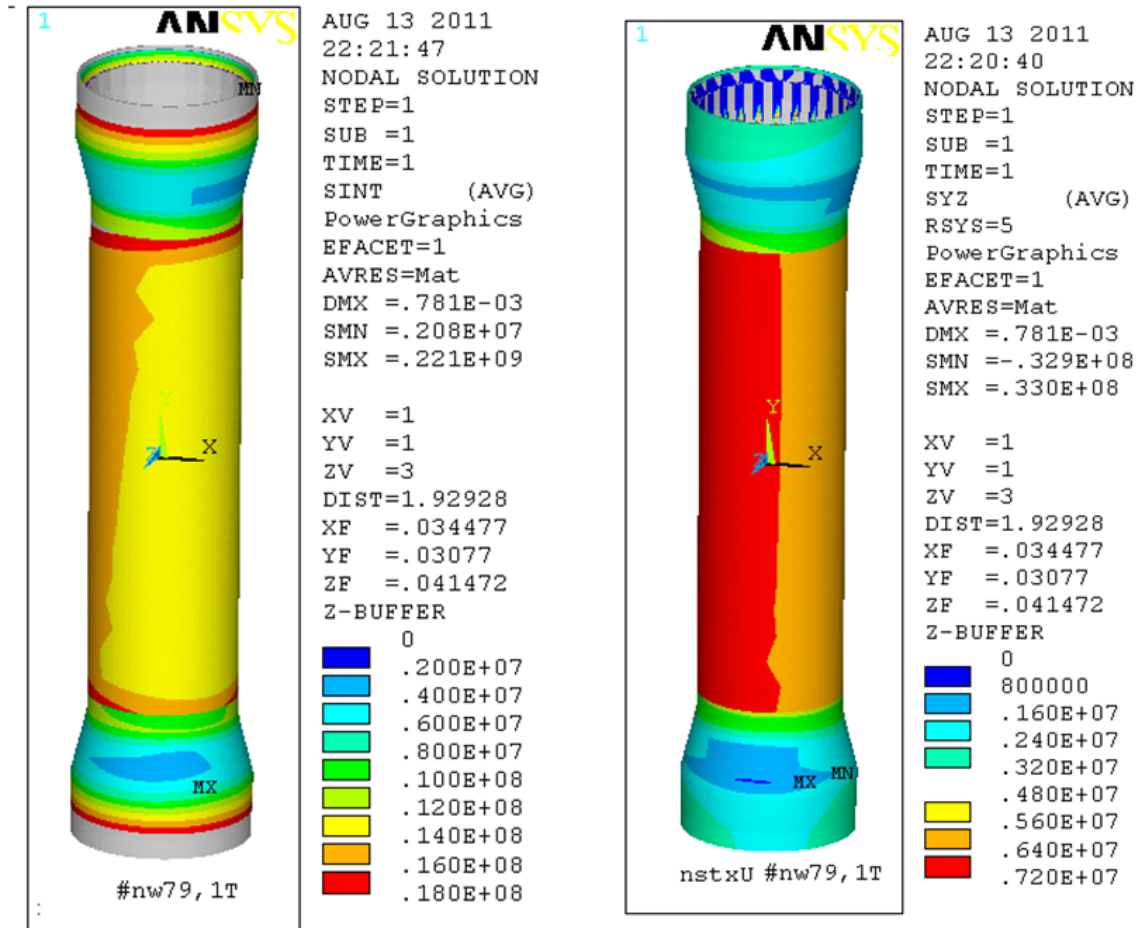


Figure 14.0-1 Torsional shear stresses

There is a torque from the TF out-of plane (OOP) loading that is transmitted through the bolted and welded connections. This has to be derived from the global modeling of the tokamak. The torsional shear stress in the casing is 6.4 MPa . Based on uniform shear flow, this would be a torque of $6.4e6/6895*.25*22.29*2*pi = 32499$ in-lb.

15.0 Seismic Loading Results

More detailed seismic analysis may be found in Reference [12]. In ref [12], both response spectra and static analyses were used. The results are approximately equivalent in terms of the magnitude of stresses.

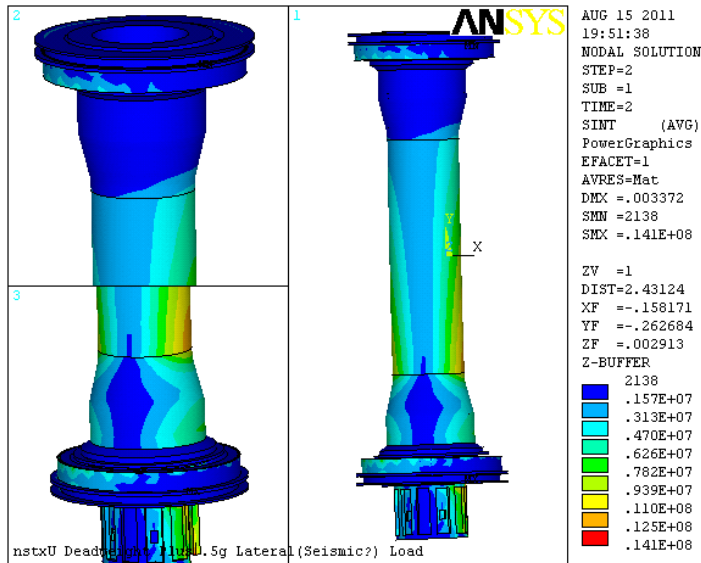


Figure 15.0-1 Casing Results for 0.5g lateral static accelerations, Global model run #32

Figure 15.0-1 shows the stresses for a later global model analysis, run#32, with a static lateral acceleration of 0.5 g's applied. The centerstack casing seismic stresses are small.

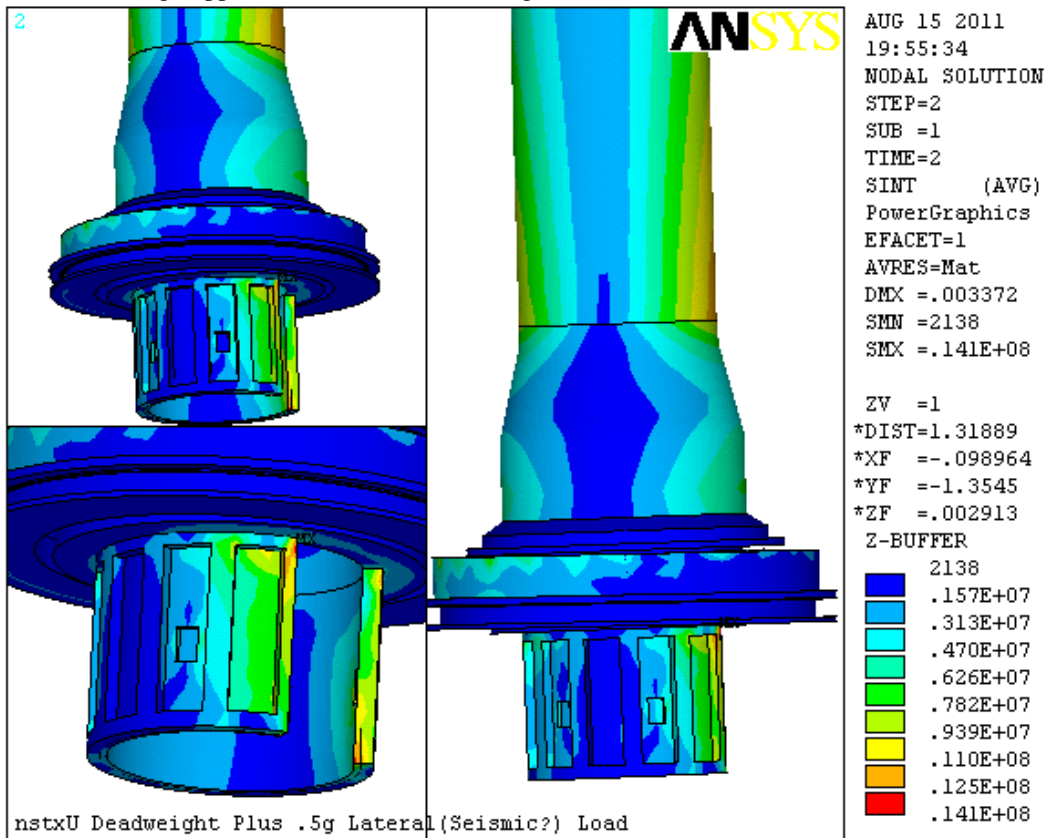


Figure 15.0-2 Skirt Results for 0.5g lateral static accelerations, Global model run #32

16.0 Lower Skirt Normal Operating Stress

The skirt is a bolted assembly. It is included in the global model in a fully merged approximate manner. The stress levels are not large and it is assumed that the local details of the skirt will not add significantly to the stresses found in the global model. Figure 16.0-1 shows the general arrangement. Figure 16.0-2 shows the treatment of the skirt in the global model.

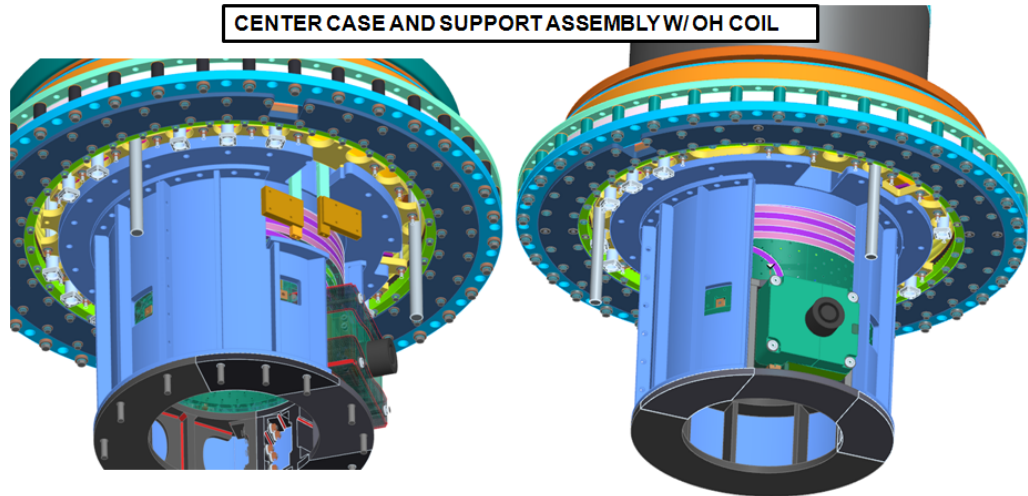


Figure 16.0-1 Views of the Lower Skirt and Penetrations for Services

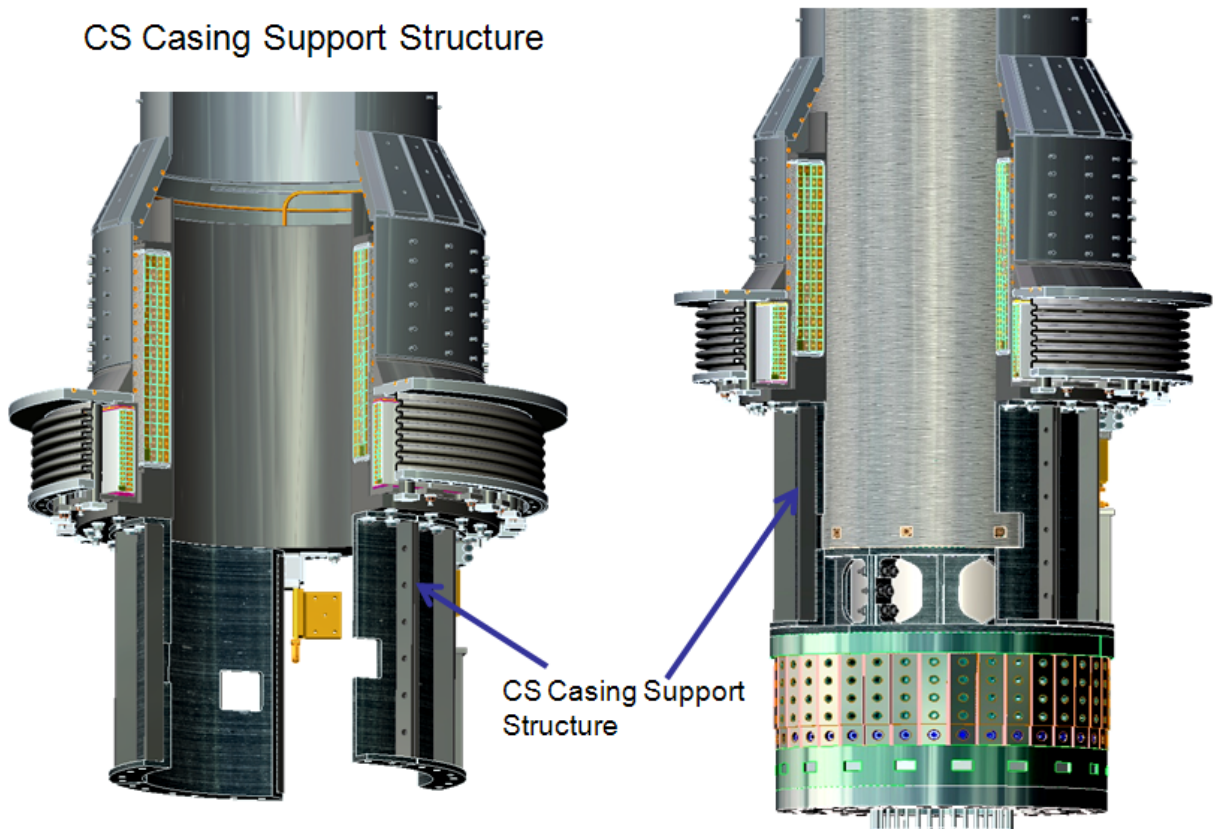


Figure 16.0-2 Views of the Lower Skirt and Penetrations for Services

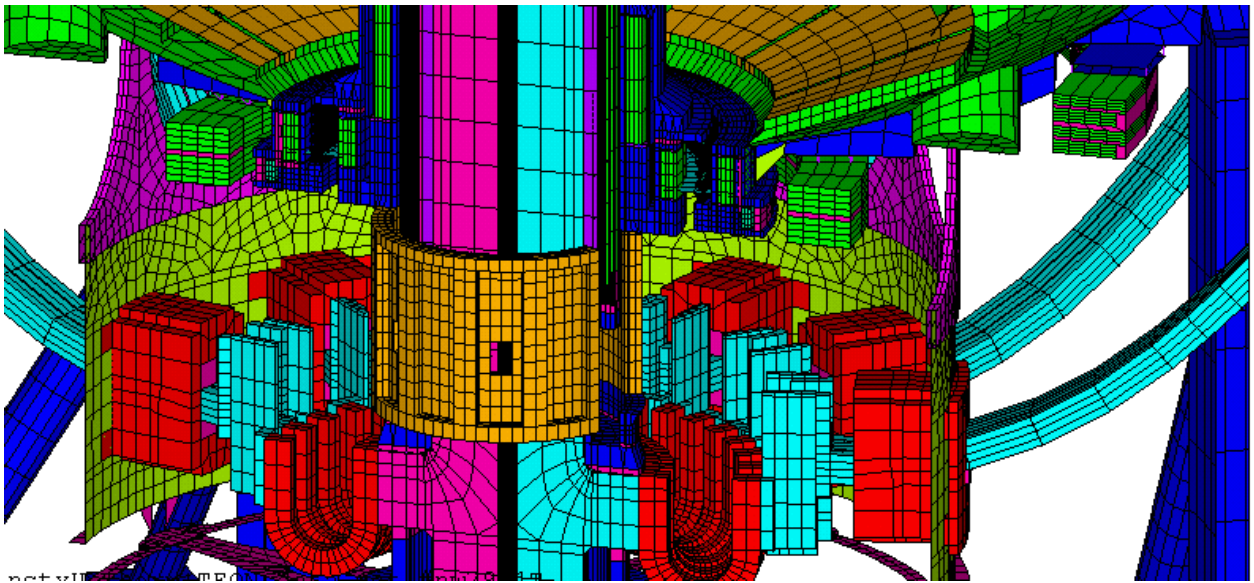


Figure 16.0-3 Lower Skirt Modeling in the Global Model

Thicknesses and flange details are represented in the global model. This design represents a major improvement in the original design of the centerstack casing support. Initially, support was via three legs which experienced excessive bending. These were replaced with the skirt assembly which had a substantially increased load carrying capability.

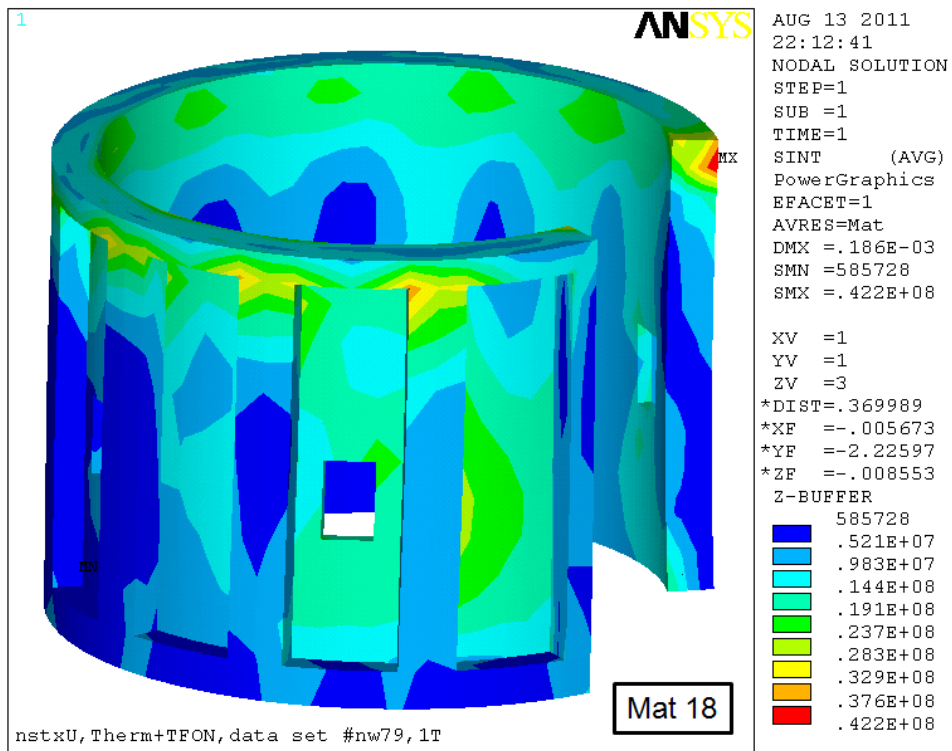


Figure 16.0-4 Lower Skirt EQ79 Stress from in the Global Model Run#34

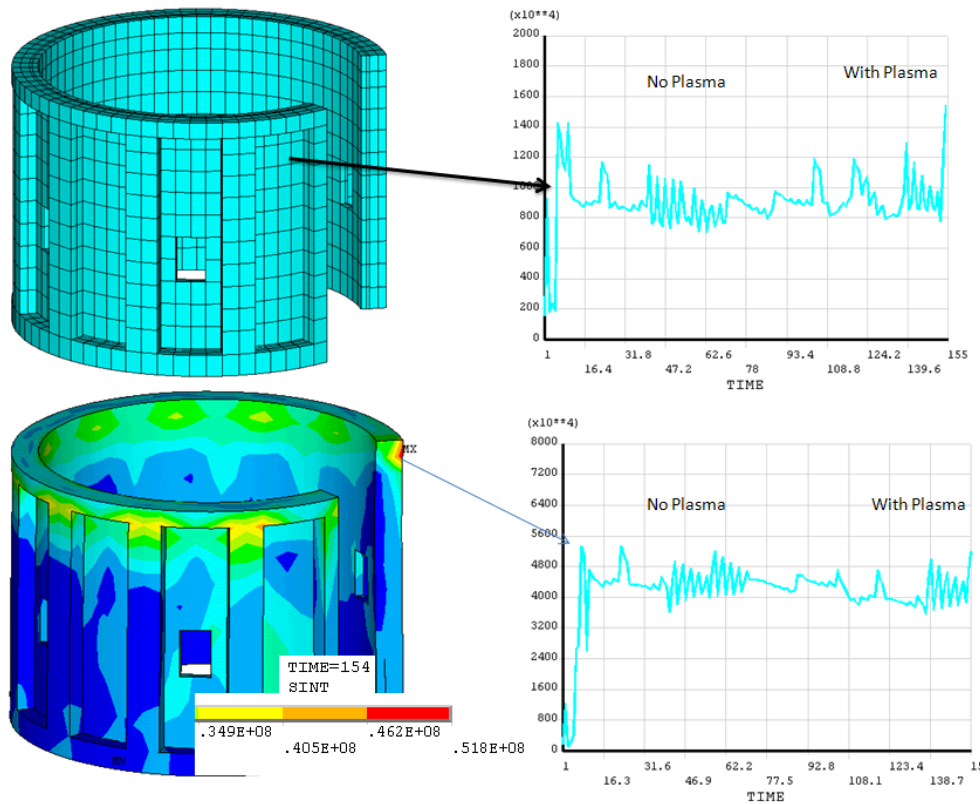


Figure 16.0-5 Lower Skirt Stress from the Global Model Run#32 for 96 no-plasma equilibria and about half off the with-plasma equilibria

17.0 Lower Casing and Skirt Bolt Stress

The lower casing support elements are loaded by the net loads from the PF Lorentz forces and occasionally from disruption halo loads imposed on the casing. Bellows loads from the expansion of the casing put compressive loads on the lower structures. This section is mainly concerned with tensile loads on the bolts and welds. The bellows compression offsets the bolt and weld tension and is conservatively ignored. There is a torque from the TF out-of plane (OOP) loading that is transmitted through the bolted and welded connections. This has to be derived from the global modeling of the tokamak and is discussed in section 14 of this calculation. The torsional shear stress in the casing is 6.4 MPa. Based on uniform shear flow, this would be a torque of $6.4e6/6895 \cdot .25 \cdot 22.29 \cdot 2 \cdot \pi = 32499$ in-lb.

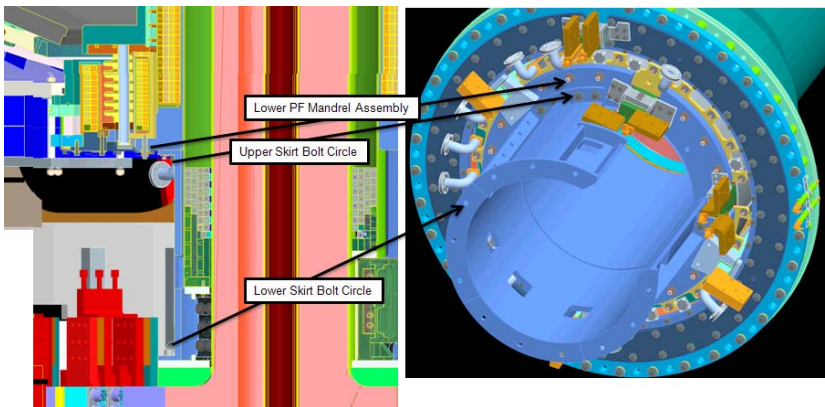


Figure 17.0-1 Three Bolt Circles are of Interest

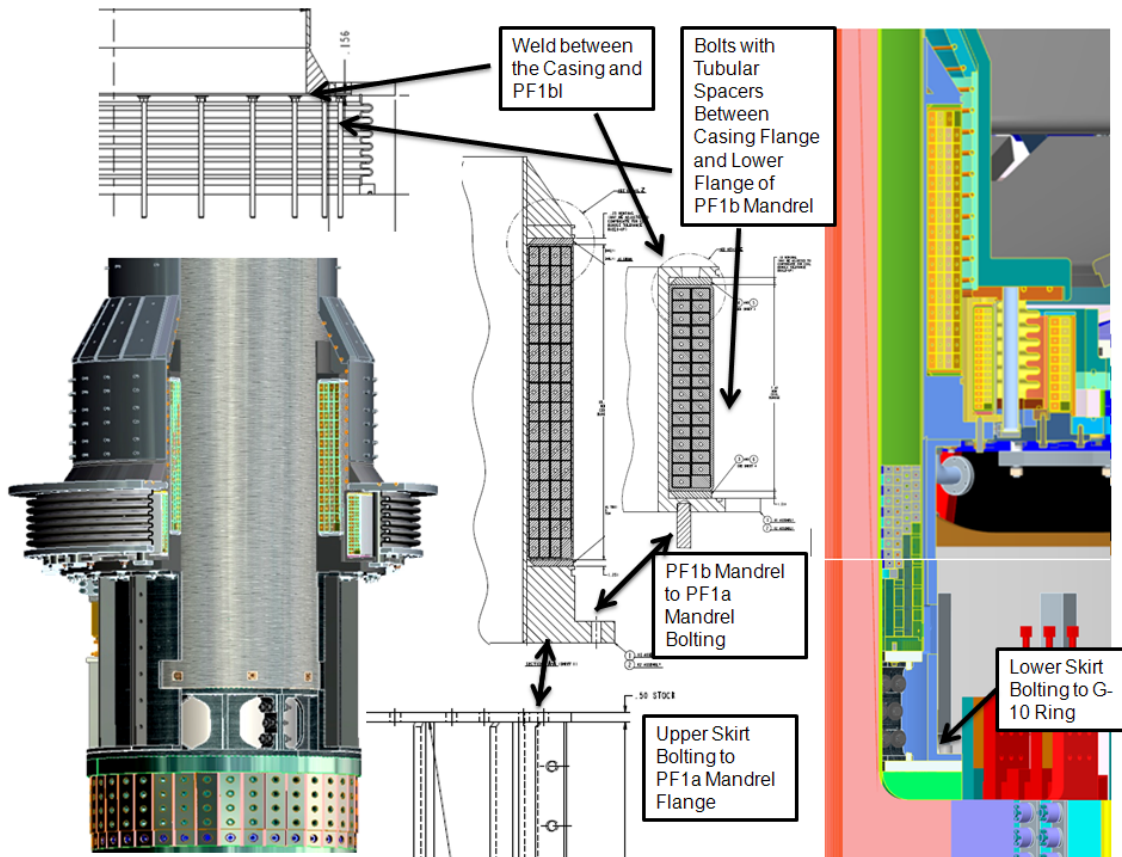


Figure 17.0-2 Another Attempt to Trace the Load Path of the Casing Supports

17.1 Upper Pf1bl Mandrel Bolting and Weld

The casing flange or divertor flange sits on the PF1b mandrel. The flange and mandrel are welded together and that weld is the primary load carrying element that supports the casing loads. As of August 16, 2011, this weld hadn't been detailed. Additionally, there are studs that connect across the outside of the mandrel that provide a redundant load path. Spacers were added between flanges connected by the studs and the studs will not load in compression. The studs act to reduce mandrel flange motion under the case loads, and share loads with the welds.

PF Mandrel Assembly Bolting

In the following spreadsheet calculation, two calculations are presented. The first assumed the studs take the moment and tensile loads. The second assumes the weld takes the loads. The weld is the stronger and stiffer of the two load paths and will take most of the loading. The studs and spacers are mainly intended to minimize flexure of the mandrel that might load the coil.

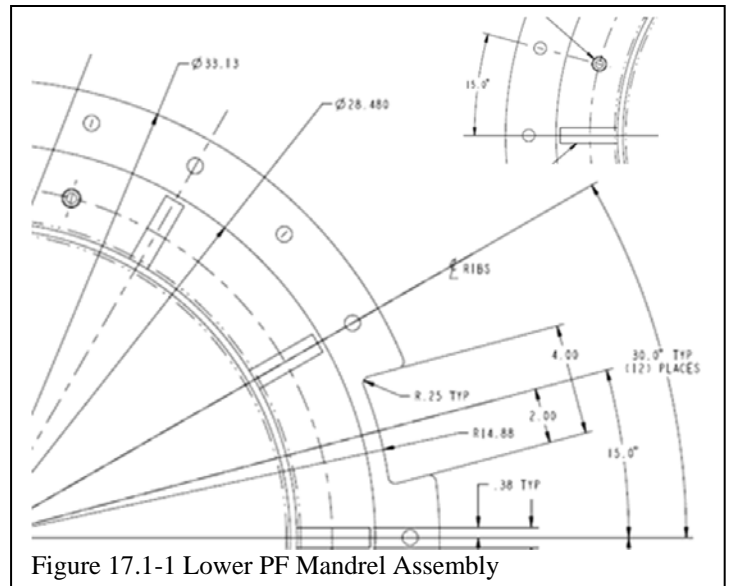


Figure 17.1-1 Lower PF Mandrel Assembly

Upper PF1b Flange Bolt Pattern and Weld to the Casing

			in/in-lbs		N/N-m		
Bolt Diameter	0.375		Halo Moment =		95000	N-m	
Bolt area	0.110446875		Halo Lateral Force =		125000	N-m	
			Halo Vertical Force =		60000	N	
			Design Point Vertical =		111926.1566	N	
			DesignPointFz	25161		lbs	
			Mom due to TF OOP	32499			
	Bolt Diameter	Bolt Stress Area	Radius	(r*cos)^2*da			
	Inches	Inches^2	inches				
0	0	1	0	15.4025	0		
1	15	0.965926	0.5	0.0773	15.4025	17.10997372	
2	30	0.866025	0.5	0.0773	15.4025	13.75379599	
3	45	0.707105	0.5	0.0773	15.4025	9.169176611	
4	60	0.499998	0.5	0.0773	15.4025	4.584566255	
5	75	0.258816	0.5	0.0773	15.4025	1.22841318	
6	90	-3.7E-06	0.5	0.0773	15.4025	2.4743E-10	
7	105	-0.25882	0.5	0.0773	15.4025	1.228480541	
8	120	-0.5	0.5	0.0773	15.4025	4.584682928	
9	135	-0.70711	0.5	0.0773	15.4025	9.169311333	
10	150	-0.86603	0.5	0.0773	15.4025	13.75391266	
11	165	-0.96593	0.5	0.0773	15.4025	17.11004108	
12	180	-1	0.5	0.0773	15.4025	18.33842058	
13	195	-0.96592	0.5	0.0773	15.4025	17.10990636	
14	210	-0.86602	0.5	0.0773	15.4025	13.75367932	
15	225	-0.7071	0.5	0.0773	15.4025	9.16904189	
16	240	-0.49999	0.5	0.0773	15.4025	4.584449584	
17	255	-0.25881	0.5	0.0773	15.4025	1.22834582	
18	270	1.1E-05	0.5	0.0773	15.4025	2.22687E-09	
19	285	0.25883	0.5	0.0773	15.4025	1.228547903	
20	300	0.500011	0.5	0.0773	15.4025	4.584799601	
21	315	0.707116	0.5	0.0773	15.4025	9.169446054	
22	330	0.866032	0.5	0.0773	15.4025	13.75402933	
23	345	0.965929	0.5	0.0773	15.4025	17.11010844	
			Moment of Inertia		201.7231292		
			Section Mod		13.09677839		
			If Only Bolts take Load			If Only Weld Takes Loads	
			Bolt Stress due to Moment (psi)		64197.90385	psi	
			Bolt Stress due to Vertical Halo+Design Point Load		21738.56797	in-lbs	
					Weld Radius	15.25	
					Weld Thickness	0.25	
					Weld area	23.9547	
					Weld Section Modulus =	182.6546	
					Weld Stress due to Moment (psi)	4603.146	
					Weld Stress due to Vertical Load	1613.42	
					Weld Stress due to Shear (psi)	1173.047	

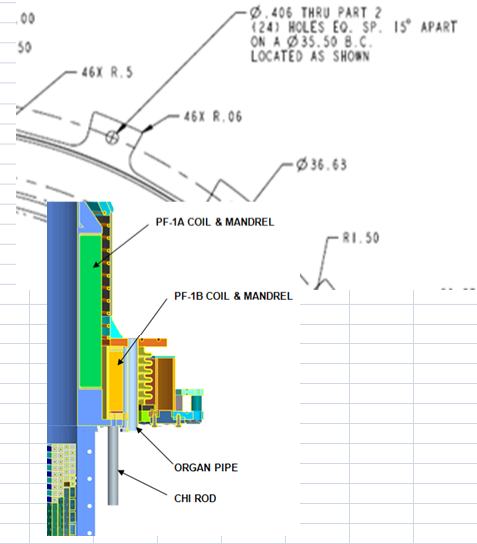


Figure 17.1-1 Upper PF Mandrel Flange and Weld Calculations

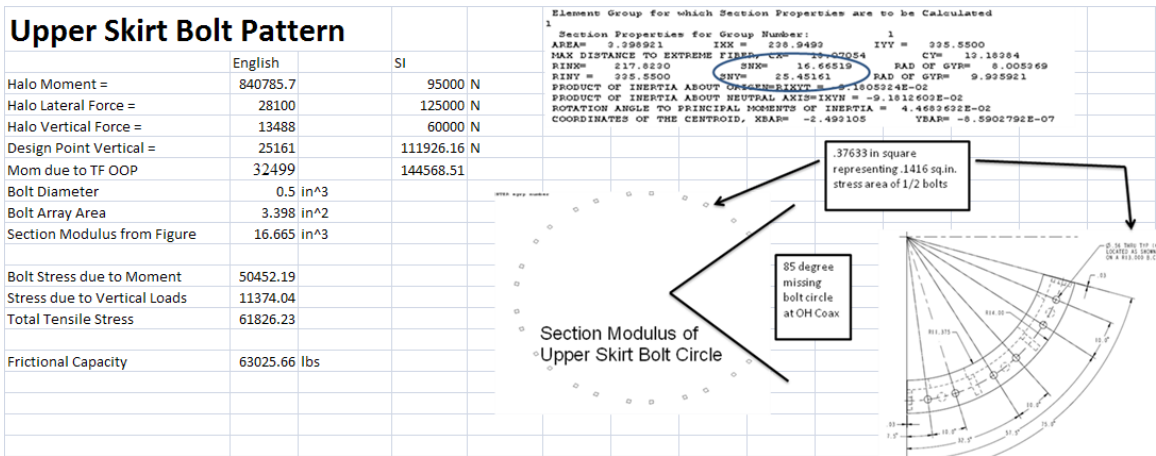
The weld stresses are low. The load path for the vertical tensile loads that result from the moment and Design Point Lorentz loads is more direct than the studs and spacers. The stud loads are overestimated in this calculation. The weld will also take the TF OOP torsional shear stress. This will be less than the 6.4 MPa (928 psi) discussed in section 14 because the PF1b Mandrel diameter is less than the central region of the casing for which the stress was quoted, and the weld thickness (1/4 inch) is the same as the casing wall thickness. Weld stresses are well below the 14 ksi allowable discussed in Figure 5.4-1.

bolts are needed. The shear capacity of the threads would actually be degraded if the welds were used. It is recommended that Loctite be used instead.

The following is an email exchange between Lew Morris and Peter Titus supporting the need for additional bolts:

Peter,
I've gone ahead and added additional studs in the available locations on the Upper and Lower PF-1B Winding Mandrels. The number of studs have increased from 21 to 34 on the Lower Mandrel and from 22 to 36 on the Upper Mandrel. Do you need the drawings for specific locations of the studs?
In lieu of Loc-tite on the threads, Jim would like to incorporate a tack weld. This should have no effect on the integrity of the High-strength bolts/studs. Do you agree?
Thanks. Lew

I calculated 20,800 shear for the threads in the lower PF1b flange. I must have miscounted but I had 23 studs. The allowable for the 316 flange is 16 ksi. The shear area was based on a strong bolt in a soft hole. I have been recommending ASTM A193 B8M class 2 bolts which are a work hardened 304 bolt, so with corrections on bolt numbers, the shear would be $20,800 * 23 / 34 = 14$ ksi; so 34 bolts is OK. But if the weld softens the stud, I lose on the shear area. The fed screw fasteners standard allows 0.75 of the hole shear area for strong studs in soft holes vs. 0.5 for soft studs in soft holes. If the whole stud was annealed, stresses would not be acceptable. A tack weld shouldn't anneal much of the stud but I am not sure. I have seen tack welds on nuts outside the stressed thread region, but never near a stressed region of a threaded fastener. I would definitely prefer Loctite. Also at installation, the studs need to be preloaded to improve the moment carrying capacity. With the 34 screws, the studs should be preloaded to 3000 lbs. Peter



The ASTM A193 B8M Class 2, 5/8-inch bolts would have a stress allowable of the lesser of $125/2$ or $2/3 * 100 = 62.5$ ksi, so they are just acceptable for this bolt pattern. The bolts should be preloaded to 75% yield, and this increases the effective section modulus of the bolt pattern. The preloaded bolt friction capacity was calculated based on a friction factor of 0.3 and there is a factor of safety of $63,025/28,100 = 2.24$ against slippage due to the lateral halo loading.

17.4 Lower Skirt Bolt (section of a) Circle

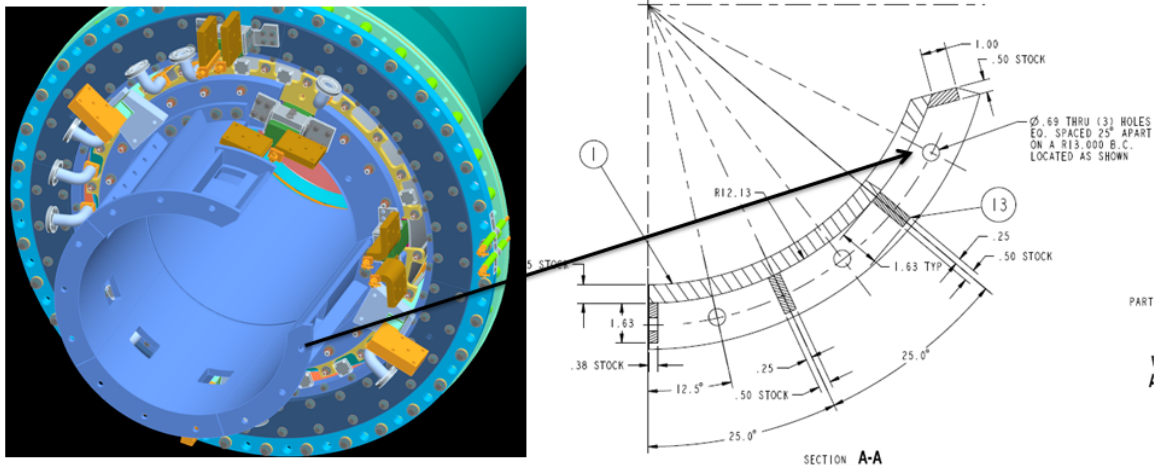


Figure 17.4-1 Layout of the Lower Skirt Flange

The skirt bolting is missing a 60-degree section corresponding to the 40-degree opening provided for the OH coax connection. In the initial set of reaction forces provided by Art Brooks, the halo loads were applied at the top of the skirt and had to be translated to the lower bolted flange section which is 22.096 inches below the upper flange. In the latest transmittal of loads (Appendix B, ref [19]) the loads are provided at the base of the skirt. In this transmittal, the lateral load is 160,000N or 36,000 lbs. The lower bolt pattern of the skirt is different than the upper pattern. There are 11, 5/8-inch bolts in the lower circle. ASTM A193 B8M class 2 bolts with 100 ksi yield are recommended. The bolts should be pre-tensioned to 75% yield. 5/8-inch bolts have a stress area of .2256 in² so this would be a load of 16,920 lbs each. Based on a friction factor of 0.3, 11 bolts would have a shear capacity of $11 * .3 * 16,920 = 55,836$ lbs, well in excess of the 37,092 lbs applied shear.

So far, the peak halo vertical tensile forces have been considered to act concurrently with the peak halo moment. A review of Art Brooks plots (Appendix B) shows that the peak moment occurs after the peak vertical load.

```

sect
Element Group for which Section Properties are to be Calculated
1
Section Properties for Group Number: 1
AREA= 2.707504 IXX = 189.7662 IYY = 267.9034
MAX DISTANCE TO EXTREME FIBER, CX = 10.42278 CY = 13.23526
RINX = 172.8089 SNX = 13.91064 RAD OF GYR = 7.989111
RINY = 267.9034 SNY = 20.24164 RAD OF GYR = 9.947286
PRODUCT OF INERTIA ABOUT ORIGIN=RIXYT = -2.3036434E-02
PRODUCT OF INERTIA ABOUT NEUTRAL AXIS=IXYN = -2.3851950E-02
ROTATION ANGLE TO PRINCIPAL MOMENTS OF INERTIA = 1.4371121E-02
COORDINATES OF THE CENTROID, XBAR= -2.502619 YBAR= -2.2897807E-06

```

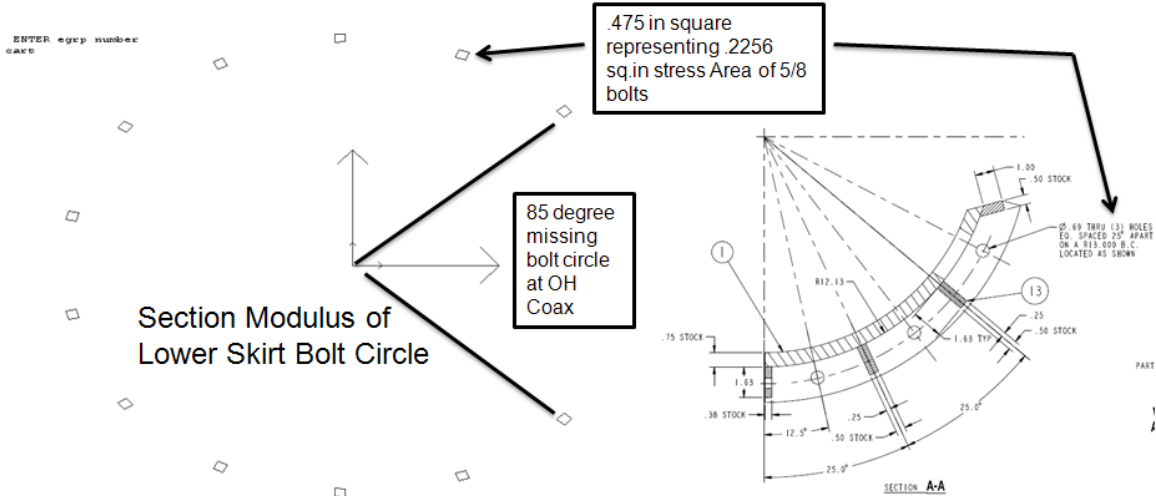


Figure 17.4-2 Section Modulus of the Lower Skirt Flange Bolting

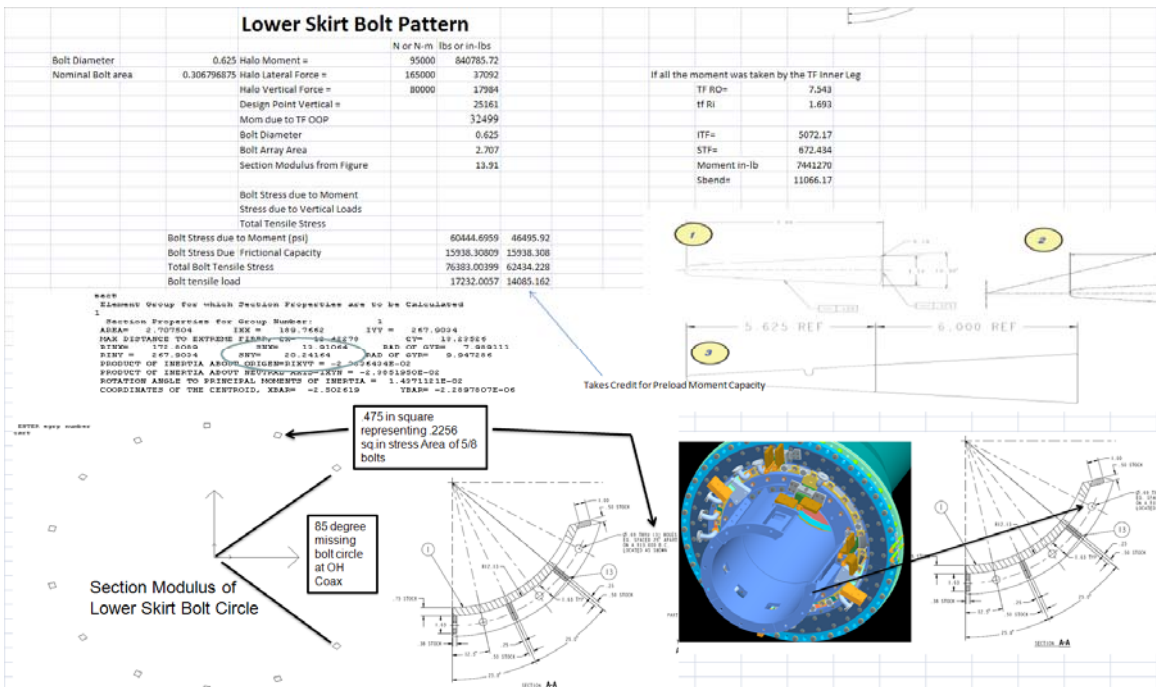


Figure 17.4-3 Lower Skirt Flange Bolt Stress Calculations

17.5 Bolt Loads on the Lower TF Flag Keys

The G-10 ring on top of the TF flags in the bottom of the machine is attached using countersunk bolts and thread inserts to the TF flags. The centerstack skirt and the OH bottom cage flange are, in turn, attached to the G-10 using bolts and thread inserts into the G-10 ring at a more radially-outward bolt pattern. Figure 17.5-1 and 2 show this interface.

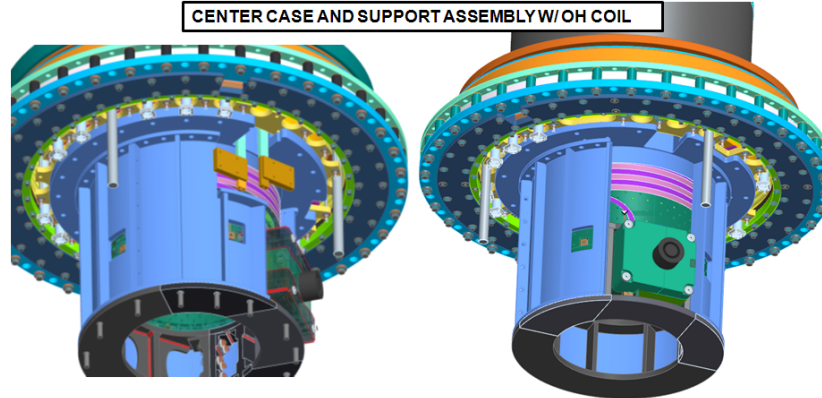


Figure 17.5-1

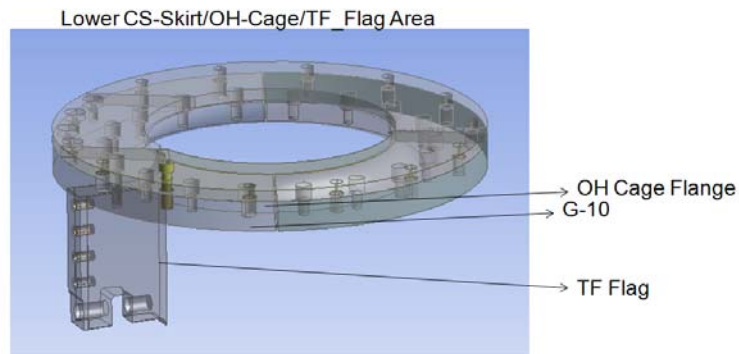


Figure 17.5-2

The OH Coax Box is analyzed in ref [23]. The OH rests on a "cage" that also is bolted into the stacked flanges above the TF flag keys. The OH is not loaded laterally. Ref [20] considers the net vertical Design Point combined OH and Inner PF loading. Additional loads from the lateral and vertical halo loading on the casing must be considered in ref [20]. The stack up of flanges, the structure around the coax, and the OH support cage are assumed to bridge the open section of the skirt.

Lower Flag Key Bolt Pattern			
Bolt Diameter	0.625	Halo Moment =	95000 840785.72
Nominal Bolt area	0.306796875	Halo Lateral Force =	165000 37092
		Halo Vertical Force =	80000 17984
		Design Point Vertical =	0 25161
		Mom due to TF OOP	0
		Bolt Diameter	0.625
		Bolt Array Area	4.06
		Section Modulus from Figure	25
		Bolt Stress due to Moment	33631.4288
		Stress due to Vertical Loads	
		Total Tensile Stress	
		Bolt Stress due to Moment (psi)	33631.4288 25870.33
		Bolt Stress Due Frictional Capacity	10626.84729 10626.847
		Total Bolt Tensile Stress	44258.27609 36497.177
		Bolt tensile load	9984.667086 8233.7632

Figure 17.5-3 Lower Flag Key Loading

The bolt load at the lower flag key is calculated to be 9984 lbs without taking credit for the preload moment capacity. This is less than the 12000 lbs considered in ref [20].

Appendix A - Email Data

From A Brooks Sept 19 2011
Peter,

The latest dynamic reaction loads to the support are significantly different from what you have (see the updated calculation of Halo Currents I sent you last week). The peak reaction loads are (from figures 23 and 24 for Fast Quench):

Fx (Lateral force)	150,000 N
Fz (Vertical force)	110,000 N
My (Moment about base)	90,000 N-m

The vertical force appears to come from a Poisson effect with the large radial forces and resulting hoop stresses in the mid section of the CS. This produces large Sz (vertical stress) which reacts at the base during the dynamic response.

The lateral force is still lower than the 50,000 lbs (222,000 N) Mark was using.

Art

Peter,

Comments on the Centerstack Casing Stress Summary Calc:

- 1) Peak stresses in CS from Halo are now reported to be 43.7MPa, down from previous 59.6 MPa
- 2) Peak Thermal Stress has dropped to 192 MPa from 280 MPa

Art

Attached is an update to the forces and moments on the CS Base Support and Bellows. The net applied load is 250 kN, up from the 140 kN previously reported. This is due to the guidance from Stefan to adjust the TPF at the strike point such that the TPF at the midplane is 1.35 (the strike point needed to be increased to 1.60). The 250 kN is very close to the estimated value obtained by assuming a constant TPF of 1.35 over the +/- 0.6m height.

The peak moment is now 130 kN-m and the peak reaction load is 250 kN at the base support. There is also a sizeable reaction at the bellows/bumper, 220 kN, though it is not in phase with the reaction load at the base (see last two figures in attached).

Art

Thu 3/11/2010 8:21 AM

Peter,

Summing up the applied halo forces for the resistive distribution scenario (for the strike at z=+/-0.6m) with PF and TF (1/R) fields I get:

Applied Load Sum on CS

Fx = -30695.6 N, Fy=Fz=0
Mx = 80400.7 N-m, My=Mz=0

I ran these thru a stress pass constraining all the points on the top and bottom flanges and looked at the reaction loads:

Reaction Loads on CS when Upper & Lower Flanges Fully Constrained

	Fx, N	Fy	Fz	Mx, N-m	My	Mz
Up	15347.	32464.	44662.	-40200.9	56846.7	-201.8
Low	15349.	-32463.	-44661.	-40199.6	-56848.9	201.8

The sum of the Up and Low values do add to negative the applied loads as expected. It just highlights the need to look at the reaction moments as well when considering support design loads.

Art



Appendix B

Halo reaction loads for the base skirt with the compliance of the G-10 flange modeled.

Peter,

Dec 19 2011

I've extracted the forces and moments at the interface of the base of the CS and top of the lower support. The peak vertical load is lower (~60 kN) than at the bottom of the lower support (~80 kN). The moments are about the same (~95 kN-m) but occur at different times. The numbers are extracted using fsum on the interface nodes with the lower support elements and are the total force (static + inertial + damping).

Art

In response to a request for the load at the PF1b mandrel elevation:

Peter,

Dec 22 2011

The lateral load at that elevation is ~125 kN. The plots I sent contain the transient behavior of each of the three load and moment directions.

Art

Peter,

Adding the compliant G10 plate and structure sitting on the TF flags has reduced the moment (now measure at the G10, $z=-2.7\text{m}$) to a peak of 95 kN-m during the dynamic response. The net lateral force has dropped to 160 kN. The bellows/bumper reaction drop slightly to 200 kN and again is not in phase with the reaction load at the base (see attached plots).

Art

----- Forwarded message -----

From: Arthur Brooks <abrooks@pppl.gov>

Date: Tue, Nov 1, 2011 at 12:31 PM

Subject: Halo Reaction Forces with Bumper

To: Peter Titus <ptitus@pppl.gov>

Peter,

